State of the Art of Single-Walled Carbon Nanotube Synthesis on Surfaces

*Yabin Chen, Yingying Zhang, Yue Hu, Lixing Kang, Shuchen Zhang, Huanhuan Xie, Dan Liu, Qiuchen Zhao, Qingwen Li, and Jin Zhang**

Single-walled carbon nanotubes (SWNTs) directly synthesized on surfaces are promising building blocks for nanoelectronics. The structures and the arrangement of the SWNTs on surfaces determine the quality and density of the fabricated nanoelectronics, implying the importance of structure controlled growth of SWNTs on surfaces. This review summarizes the recent research status in controlling the orientation, length, density, diameter, metallicity, and chirality of SWNTs directly synthesized on surfaces by chemical vapor deposition, together with a session presenting the characterization method of the chirality of SWNTs. Finally, the remaining major challenges are discussed and future research directions are proposed.

1. Introduction

Structure determines properties. Carbon element can form many different kinds of low-dimensional allotropes, including C_{60}, carbon nanotube (CNT) and graphene. CNT, as a typical one-dimensional nanomaterial, possesses unique chiral structure and superior properties. During the past two decades, CNTs have drawn great attention due to their superior electrical, thermal, mechanical properties and numerous promising applications in many fields.[1–4] Particularly, single-walled CNTs (SWNTs), with their fascinating electronic properties, are one of the most attractive candidates to be used as building blocks in the next generation nanoelectronics. Plenty of functional nanodevices based on SWNTs, such as the elemental p-type and n-type field effect transistors,[5,6] and integrated ring oscillator,[7] have been continuously emerged. And very recently, a CNT computer[8] with its central processor entirely based on CNTs has been demonstrated, further proving the potential of CNTs to replace silicon-based semiconductors. Towards their practical applications, the large scale and controlled synthesis of SWNTs is the first step. Since its discovery in 1993,[9,10] various methods, including arc-discharge, laser ablating method and chemical vapor deposition (CVD), have been developed to produce SWNTs. Among these methods, CVD is the most promising one which could produce SWNTs with large-scale and low-cost.[4] SWNTs could directly grow on the surface of a substrate, which will greatly facilitate the fabrication of SWNT-based nanoelectronics. The structural similarity of the various SWNTs makes their controlled synthesis with great challenges. In addition, the properties of SWNTs highly depend on their chiral structures, such as the diameter, length, and chirality. Therefore, structure controlled growth of SWNTs, especially directly on surfaces, are highly desired for the fabrication of SWNT-based electronics.

The structure of a SWNT can be viewed as a seamless rolled up graphene. Depending on the rolling vector, the SWNTs could have varied diameters (d), chiral angles (θ) and handedness (right-handed (R) and left-handed (L)). **Figure 1** shows that a graphene layer could be rolled up along different directions and form SWNTs with similar diameters but different chiral structures. The rolling vector (n, m) can be used to describe the structure of a SWNT, including its diameter and chirality. Besides, the length of SWNT is also a very important structural characteristic. For SWNTs on a substrate, their relative orientation and areal density on the surface are also crucial factors, determining the density of the fabricated electronics. During the past, great efforts have been paid to control the diameter, chirality, alignment, length, and the density of as-grown SWNTs on surfaces, and many exciting achievements have been made. At the same time, many unsolved problems still remain and need further effort.

In this review, we first present the main aspects of the CVD growth process of SWNTs on surfaces. Then, the progress in controlling the orientation (alignment), the length, the areal density, the diameter, the conductive type, and the chirality

Y. B. Chen, Y. Hu, L. X. Kang, S. C. Zhang, D. Liu, Q. C. Zhao, Prof. J. Zhang
Center for Nanochemistry
Beijing National Laboratory for Molecular Sciences
Key Laboratory for the Physics and Chemistry of Nanodevices
State Key Laboratory for Structural Chemistry of Unstable and Stable Species
College of Chemistry and Molecular Engineering
Peking University
Beijing 100871, P.R. China
E-mail: jinzhang@pku.edu.cn
Dr. Y. Y. Zhang, H. H. Xie
Center for Nano and Micro Mechanics
Tsinghua University
Beijing 100084, P.R. China
L. X. Kang, Prof. Q. W. Li
Suzhou Institute of Nanotech and Nanobionics
Chinese Academy of Sciences
Suzhou 215123, P.R. China

DOI: 10.1002/adma.201400431

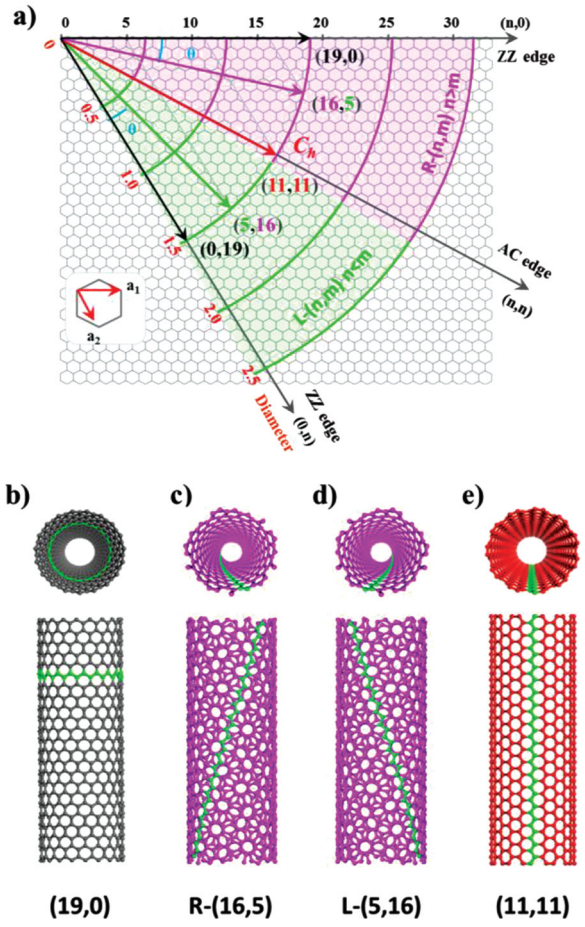

Figure 1. Illustration for the structure of SWNTs. (a) A graphene layer could be rolled up along different directions to form SWNTs with different chirality. (b-e) SWNTs with similar diameters but different chiral structures, including zigzag tube (19,0), right-handed chiral tube (16,5), left-handed chiral tube (5,16), and armchair tube (11,11).

during the growth of SWNTs will be reviewed. There are still big challenges toward the chirality controlled growth of SWNTs, for which, the facile characterization of chirality is of importance. For this purpose, the progress in the determination of chirality is also included. Finally, we conclude the challenges and opportunities for future research toward the structure controlled growth of SWNTs.

2. CVD Growth of SWNTs

Developing controlled growth method toward SWNTs with uniform structures and properties is the key to advance practical applications of SWNTs in many fields. In the past twenty years, several methods have been developed to produce SWNTs, among which CVD is the most promising method for large scale production of SWNTs. CVD has advantages of mild synthesis condition, simple facility, high yield and low cost. In a CVD process, the structures of SWNTs are strongly affected by parameters such as temperature, substrate, precursors and catalyst. In this part, we will overview the process of the synthesis of SWNTs on surface by CVD. Based on this, we will also discuss the relationship between catalysts and SWNTs.

2.1. Synthesis of SWNTs on Surfaces

Various synthesis approaches have been developed since the discovery of SWNTs. Arc discharge[11] and laser ablation[12] are

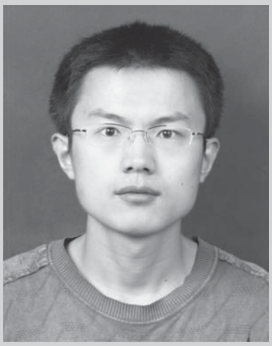

Yabin Chen was born in Hebei province, China. He received his B.S. from Lanzhou University in 2008. Since then, he joined Prof. Jin Zhang's group for a 5-year Ph.D. program at Peking University. His research interest mainly focuses on the preparation and properties of low-dimensional nanomaterials, including the structure controlled growth of SWNTs and their related applications. Now, he is a postdoc researcher at the University of California, Berkeley.

Yingying Zhang received her Ph.D. degree in chemistry from Peking University in 2007. After a three-year postdoctoral fellowship in Los Alamos National Laboratory (USA), she joined the Center for Nano and Micro Mechanics (CNMM) in Tsinghua University as an associate professor in 2011. Her research is focused on the controlled synthesis, assembly and composites of carbon nanotubes.

Jin Zhang received his Ph.D. from Lanzhou University in 1997. After a postdoctoral fellowship at the University of Leeds, UK, he joined to Peking University where he was appointed Associate Professor (2000) and promoted to Full Professor in 2006 and Chang Jiang Professor in 2013. His research focuses on the controlled synthesis and spectroscopic characterization of low-dimensional carbon materials. Currently, he serves as the editor of *Carbon*.

the earliest techniques for successful SWNT growth. These two methods played important roles in the preparation of carbon nanomaterials, including SWNTs. However, the process through arc discharge and laser ablation is hard to control. Powder-like SWNTs obtained through these two approaches are limited in the application of electronics due to the lack of effective dispersion and processing strategies. Furthermore, some high-end applications such as nanoelectronics and field emission, require SWNTs on patterned surfaces or in special orientations. These needs could be satisfied through CVD growth of SWNTs. A conventional CVD system usually uses a resistive or inductive heater as the heat source, being called as thermal CVD. According to the pressure in the CVD process, CVD is classified as atmospheric-pressure CVD (APCVD) and low-pressure CVD (LPCVD). Besides, plasma-enhanced CVD (PECVD), where a plasma source is used to enhance the reaction, is also widely used. As schematically illustrated in **Figure 2**a, the process of CVD is a catalytic conversion of a gaseous precursor at high temperatures into a solid material at the surface of catalyst particles.[13,14] During this process, the factors influencing the structures of SWNTs could be analyzed through the interaction of gas, catalyst, substrate, and the SWNT, as shown in Figure 2b. I1 to I6 symbolize the interactions between each two factors. These factors are interrelated and affect the structures of SWNTs together.

In the CVD growth of SWNTs, there are many factors affecting the structures of the SWNTs, leaving plenty of space for the structure controlled growth of SWNTs. For examples, a large number of carbon precursors including gaseous molecules,[15] and liquid molecules,[16] such as carbon monoxide, methane, acetylene, ethylene, alcohol, benzene and cyclohexane, can be selected for the growth of SWNTs. Many materials, including metallic and non-metallic, could be used as the catalysts for SWNTs. Besides, if we want to synthesis SWNTs directly on surfaces, many kinds of single crystals and amorphous substrates can be used. Furthermore, the temperature, atmosphere and pressure in CVD process could be continuously adjusted, which lead to many opportunities for the controlled growth of SWNTs through CVD method. In the following, the catalysts for the SWNT growth and the mechanism for the formation of SWNTs will be reviewed.

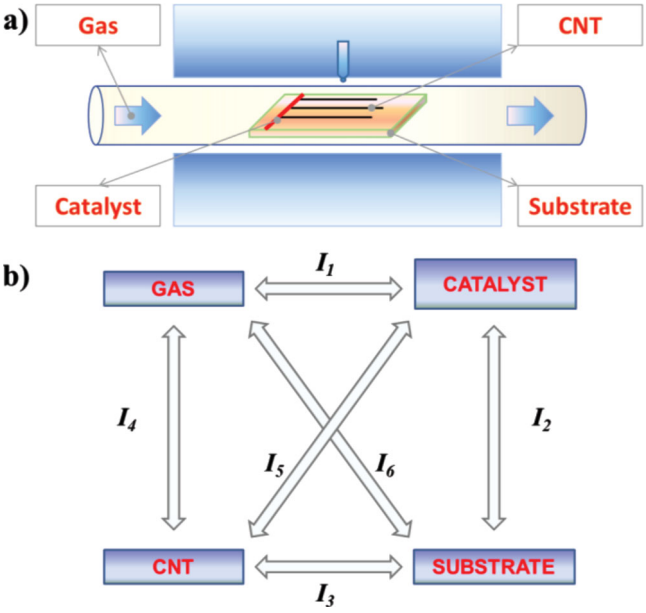

Figure 2. Illustration for the CVD process of SWNT growth. a) General growth process of SWNTs in CVD. b) The interaction of various factors in the growth of SWNTs. I_1 to I_6 symbolize the interactions between each two factors.

2.2. Catalysts for the CVD Growth of SWNTs

Catalysts are an extremely important factor affecting the structures of SWNTs.[17–31] Generally speaking, the size and the crystalline structure of catalyst nanoparticles influence the number of walls,[22] diameter[32] and chirality of SWNTs. The catalytic activity and life of the catalysts determine the growth rate[26] and the length of SWNTs, respectively. The relative locations of catalyst nanoparticles determine the distribution and alignment of the produced SWNTs.[33,34]

A variety of metal elements could be used to catalyze the CVD growth of SWNTs. Iron-family elements such as Fe, Co, Ni and their alloys, which have the catalytic function of graphite formation,[17] are the most commonly used catalysts for the growth of SWNTs. Au, Ag, Pt and Pd, as nobel metals can also be used as the catalysts for the growth of SWNTs.[18] Carbon atoms can be dissolved in both iron-family metals and noble metals though their binding energies are different. Then carbon atoms precipitate for the growth of SWNTs. Besides, many other elements, such as Cu, Mn, Mo, Cr, Sn, Mg, and Al, have been proved to be suitable to catalyze the growth of SWNTs.[19]

However, the existence of thick graphite layers encapsulating metal nanoparticles severely limit the application of SWNTs in many fields.[20] In order to resolve problem of the residual metallic catalysts, non-metallic nanoparticles have been investigated as the catalysts for SWNT growth. The first clear evidence of non-metallic catalyst growth of SWNTs was observed on 6H-SiC surface in 2002.[21] The SWNTs formed highly ordered networks on and below the surface with a narrow diameter distribution, indicating that non-metallic nanoparticles could catalyze the growth of SWNTs with controlled structures. In 2007, semiconductor nanoparticles, such as SiC, Ge, and Si, were also reported as catalysts for catalytic growth of SWNTs and double-walled CNTs in CVD using ethanol as precursor.[22] These particles have a cluster-like structure, and CNT caps form on the surface. However, many researchers did not pay much attention to non-metallic catalysts until 2009. Homma and his coworkers found that nano-diamonds can catalyze the growth of SWNTs. Similar to the vapor-solid-solid (VSS) mechanism for the growth of semiconductor nanowires from a solid particle,[23] the formation of SWNTs from nanodiamonds occurs via the so-called vapor-solid surface-solid (VSSS) mechanism.[24] Carbon atoms can not be dissolved in nano-diamonds, instead, they diffuse on the surface of the nanoparticles to promote the growth of SWNTs. In the same year, Huang et al.[25] made surprising progress on the exploration of growth catalysts of SWNTs. They reported that many oxide nanoparticles including SiO_2, Al_2O_3,

TiO_2, Er_2O_3 and all lanthanide oxides except promethium oxide are active for the growth of SWNTs. They proposed that nano-sized particles are in a molten status at high temperature. The atoms can move around quickly, thus creating a space hole or dislocation which might catalyze the decomposition of hydrocarbon. The high curvature of nanometer-sized particles can be templates for the formation of SWNT caps. The further growth of SWNTs starts at the hemispherical caps.

The use of SiO_2 as a catalyst for SWNT production is of particular interest due to their potential applications in silicon-based technology. Cheng et al. found that the growth velocity of the SWNTs from SiO_2 catalyst is 300 times slower than iron group catalysts, which is only 8.3 nm/s.[26] In situ transmission electron microscopy (TEM) studies and density functional theory calculations reveal that oxygen can enhance the capture of $–CH_x$ and play an important role in the CVD process.[27]

To summarize, a large variety of nanoparticles have been confirmed to be suitable for CNT growth. Hereafter are analyzed important physical and chemical properties of the nanoparticles actually required to promote the controlled growth of SWNTs.

2.3. Growth Mechanism

To study the growth mechanisms of SWNTs is very important for the controlled growth of SWNTs. For metal catalysts, such as Fe, Co and Ni, the most well accepted mechanism is the vapor–liquid–solid (VLS) as shown in **Figure 3**a, which was first proposed as a growth model for silicon nanowires.[28] In this process, a metal catalyst particle is exposed to a hydrocarbon at elevated temperatures. Carbon sources decompose into hydrocarbon fragments. Then hydrocarbon fragments diffuse into the catalysts, and upon super saturation, the redundant carbon would precipitate into the SWNT caps along the catalyst surface.[29] Besides, some carbon atoms could bind with the edge of SWNTs directly[30] and some other carbon atoms could diffuse along the catalyst surface and contribute to SWNT growth.

In contrast, non-metallic catalysts, such as Si, diamond, and SiO_2, have very low solubility for carbon according to their phase diagrams. Takagi et al. proposed VSSS model to explain the growth of SWNTs on diamond surfaces.[24] In the environment with depletion of carbon precursors, graphite island is formed on the π-bond relaxed surface of the diamond. The curved graphite island lifts off the particle surface except its edge which acts as incorporation sites for carbon adatoms, and then the formation of SWNT is induced. Besides the VSSS growth mechanism, there are other hypotheses such as VSS[31] or VS[32] (Figure 3b). They can be understood as a surface reaction system.

For the growth of SWNTs on the surface, according to the relative position of substrate, catalyst and SWNT, tip-growth and base-growth modes have been proposed. In tip-growth mode, the active catalyst detaches from the substrate and moves forward during the growth of SWNTs, as shown in Figure 3c.[33] Base-growth mode is shown in Figure 3d.[34] In this case, the whole nanotube moves away from the catalyst while the catalyst stays in its original position. Both of these two modes have been proved by in situ TEM studies.

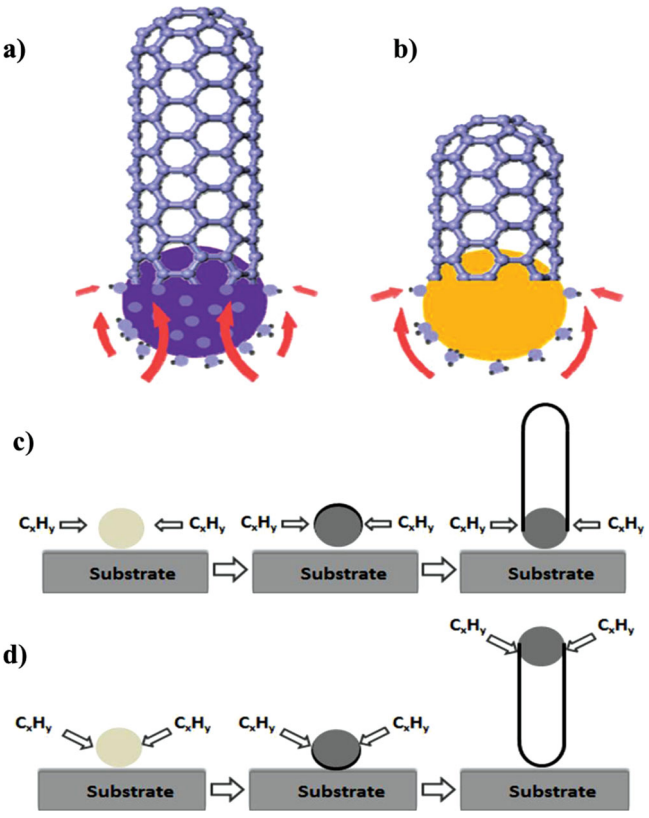

Figure 3. a) The classical VLS mechanism during SWNT growth from metallic catalyst. b) The supposed VS mechanism during SWNT growth from non-metallic catalyst. (a) and (b) are reproduced with permission.[32] Copyright 2011, Elsevier. c) The tip-growth mode. d) The base-growth mode.

Although significant progresses have been made in understanding the formation mechanism of SWNT, there are still many challenges. To synthesis SWNTs with controlled chirality, further studies on the mechanisms are required.

3. Orientation Control

SWNT arrays have been regarded as the functional building blocks for future carbon nanoelectronics owing to their superb structures and unique properties.[35,36] Comparing with the random SWNT networks, aligned SWNT arrays with the identical density can effectively preclude both the mis-oriented ones and tube-tube connections. Therefore, aligned SWNT arrays are very favorable to fabricate integrated circuits and further reveal their optimal performances.[37] For example, filed-effect transistors fabricated based on dense and perfectly aligned SWNT arrays presented the scaled transconductance and device-level mobility approximating 3000 S m^{-1} and 1000 cm^2 V^{-1} s^{-1}, respectively.[35] The scientists of IBM research center, as the longtime leader of carbon nanoelectronics, have clearly claimed that the desired SWNT arrays should be with a density of 125 nanotubes/μm and metallic impurity of less than 0.0001%.[38] Definitely, this ultimate target for SWNT sample preparation presents the tremendous challenges, and the

essential prerequisite is how to realize the orientation controlled synthesis of SWNTs. Although much effort has been devoted to the post-growth treatment for SWNT arrays, such as Langmuir-Blodgett assembly[39] and blown bubbling method,[40] the obtained SWNTs in these arrays are normally limited by the short length, adsorbed contamination and uncertain locations.[41] In contrast, the as-grown SWNTs via catalytic CVD system maintain their intrinsic chiral structures and clean surfaces, which are also compatible with the standard fabrication procedure of silicon-based devices.[37,42] Hence, it is critical to directly align SWNTs into parallel arrays during their growth. Notably, there are two kinds of SWNT arrays, horizontally and vertically,[43] according to their interrelations between the grown SWNTs and supported substrate. In this section, the former will be mainly considered.

Nowadays, the orientation controlled growth methods can be classified into three categories: gas flow directed,[44] surface structure directed[45,46] and external field assisted,[47] which are validated at the interfaces between SWNTs and gas, substrate and special field, respectively. As we know, the CVD system seems like a complex black box, and all reactive conditions are linked together to determine SWNT's structures.[48] The used substrate, gas feedstock and temperature are three elementary parameters for the growth process. Certainly, surface structures of substrate and state of gas flow can partially decide the growth orientation of SWNTs under a suitable temperature range. Surface structures contain crystallographic lattices and atomic steps, both of which can bring the anisotropic interactions to confine the SWNT's growth along the homologous directions.[49,50] Following the surface directed mode, SWNT arrays with high density are conveniently produced. In general, the gas flow directed growth mode strictly relies on a stable laminar flow and SWNT floats above the substrate,[51] so it normally works well at a higher temperature compared to surface directed mode. Moreover, external fields can be introduced to yield the applied force, which further guides the SWNT growth. For example, the electric field has already exploited to not only produce the aligned SWNT arrays, but also sort out the metallic SWNTs.[52] In addition, the different directed modes can play their individual role at one CVD batch. So, their synergistic effects can be developed to produce the complex architectures of SWNTs.[53,54] For instance, the cross-bar and serpentine SWNTs can be obtained by combining gas flow-electric field[55] and surface-gas flow directed modes,[56] respectively.

3.1. Gas Flow Directed Growth Mode

The interfacial interactions between catalyst/SWNT and its substrate can be strongly weakened with the increased temperature. At a critical value, catalyst nanoparticles would remain a floating state away from the substrate surface. As such, the aligned orientation of SWNTs is entirely controlled by gas flow, namely, gas flow directed growth mode as shown in **Figure 4**a.[57] It is well accepted that this directed mode follows the tip growth mechanism. In situ sample rotation instrument was established to investigate the detailed processes of the gas flow directed SWNTs.[58] The obtained SWNTs exhibited various morphologies by rotating the substrate during the growth process, including cross-bars, kinks, curvatures and bundles. It was also proven that the 'total' nanotube, not only upstream segment, kept above the substrate during its growth. The oscillatory motion perpendicular to nanotube axis, rather than growth termination, led to the landing of SWNT onto surfaces. Moreover, free-standing SWNTs could be prepared by using specific substrates with patterned trenches.[44] Absolutely, these two phenomena evidently corroborate the gas-flow directed mode.

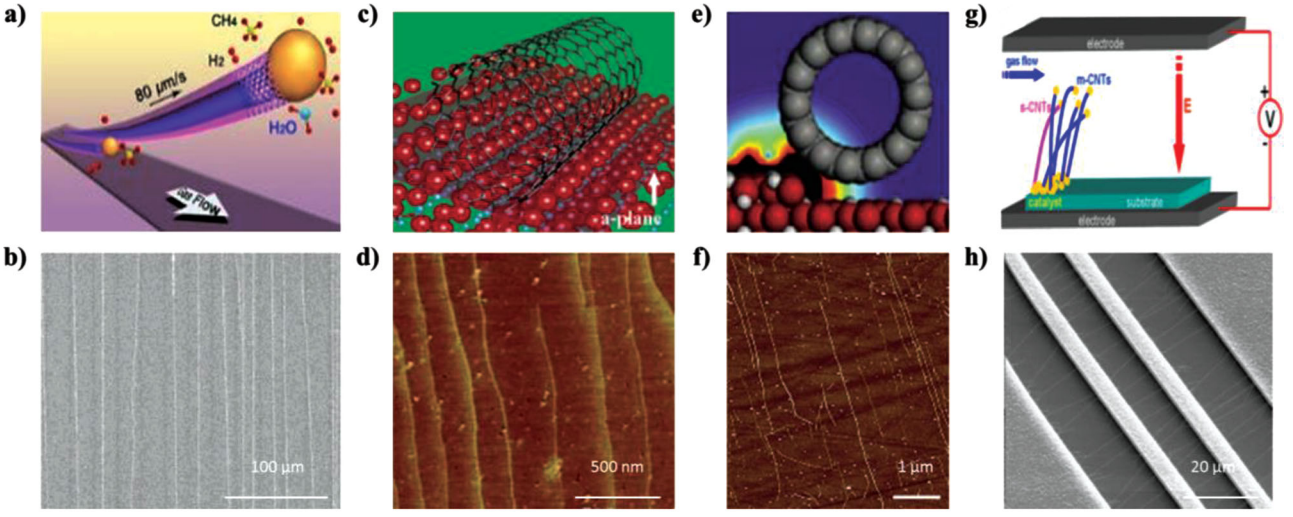

Figure 4. Orientation controlled growth methods of SWNTs. a, b) Gas flow directed growth mode and the obtained ultra-long SWNTs. (a) is reproduced with permission.[57] Copyright 2010, American Chemical Society. (b) is reproduced with permission.[59] Copyright 2007, American Chemical Society. c, d) Lattice directed growth mode and the atomic force microscopy (AFM) image of aligned SWNTs. Reproduced with permission.[49] Copyright 2005, American Chemical Society. e, f) Atomic nano-step directed growth mode and the grown SWNTs. Reproduced with permission.[46] Copyright 2004, Wiley-VCH. g, h) Electric field directed growth mode and the suspended SWNTs. (g) is reproduced with permission.[52] Copyright 2011, Elsevier. (h) is reproduced with permission.[67] Copyright 2009, Wiley-VCH.

Gas flow directed mode has advantages on the synthesis of ultra-long (Figure 4b) and suspended SWNTs with a superior growth rate.[59] The floating catalyst is fully exposed because of the absence of interaction with the substrate, which remarkably improves its lifetime and activity. In this way, Zhu et al. firstly synthesized 4 cm-long individual SWNT at a rate of 11 μm/s in 2004.[60] SWNT's length was only limited by the growth time and furnace size. Accordingly, Wei et al. successfully prepared 55 cm-long few-walled CNTs with perfect structures in a movable furnace.[61] They found that its growth rate reached up to 88 μm/s under the modified conditions, which was $T = 1010$ °C and R (H_2/CH_4) = 2. Despite many efforts, it is noticed that the density of horizontally aligned SWNTs is extremely low. It mostly originates from many complex factors, including the aggregation of nanoparticles, entanglement of short nanotubes, and advanced falling down of SWNT's tip.[62]

Catalyst–substrate interaction and flow stability are the key factors to optimize the CVD growth process. At present, the available catalysts range from metallic to non-metallic nanoparticles,[53,63] which surely displayed the different interactions with substrates. Aiming to decrease the catalyst-substrate interaction, silica nanoparticles have been dispersed on the substrate surface to promote the growth of aligned SWNTs using Fe as the catalysts.[64] Moreover, the results from molecular dynamic simulations revealed that Cu possessed the weak interactions with SiO_2 than the Fe.[65] Therefore, Cu nanoparticles were preferable to be lifted up for preparing SWNT arrays at the same temperature. Additionally, J. Zhang's group found this result also coincided on ST-cut quartz.[66] Both fast heating[51] and ultra-low feeding gas[59] are significantly profitable to stable the gas environment. As the result of fast heating, a convection flow was formed owing to the temperature difference, which could lift up some nanotubes with the catalyst. Similarly, the ultra-low gas benefited generating the steady laminar flow, which was facile for guiding the aligned ultra-long SWNT arrays.

3.2. Surface Directed Growth Mode

Surface directed growth mode essentially relies on the anisotropic van der Waals interactions between SWNT and various surface structures of substrate, including the crystallographic lattice (Figure 4c),[49,67] faceted nano-steps (Figure 4e)[46,50] and etched trenches.[68] Accordingly, it can be divided into lattice directed and nano-step directed growth modes, which are capable to prepare aligned SWNT arrays with high density. Si (100) and (110) were firstly applied to guide the growth of large-scale and horizontally aligned arrays.[45] Theoretical simulations correspondingly showed the preferable potential energy when SWNTs were along these directions. Subsequently, this kind of substrates extensively consists of Al_2O_3 (a- and r- plane), mis-cut quartz (Y-, ST-, R- and Z-cut), MgO, mica and graphene.[42] Of which, ST-cut quartz is the most widely and robustly used surface due to its remained configurations under growth temperature. Joselevich et al. fabricated numerous faceted nano-steps on the sapphire surface to regularly induce the orientation and conformation of SWNTs. The obtained SWNTs also completely reflected the atomics features on the surface, such as crystalline, facets, defects and kinks.[54] Moreover, this strategy was further generally applicable to other nanomaterials, such as GaN and ZnO nanowires.[69,70]

The mild temperature, prefect structures and suitable catalyst density are the critical requirements for surface directed growth mode. With elevated temperature, gas flow can take the place of surface to direct the SWNT. The active catalyst at the tip of SWNT becomes larger by the random colliding and merging with other nanoparticles on surface due to Ostwald ripening effect. Meanwhile, the growing SWNT can alter its orientation and form a 'sickle' shape on the basis of tip growth mechanism.[71] Besides, it is difficult to prepare surfaces with perfect structures. The annealing process is an efficient manner to reconstruct the surface atoms, and then observably improve the crystal quality, like the calcination of ST-cut quartz at the 900 °C for 8 h.[35] It is noteworthy that the SWNT growth on Al_2O_3 presented a clear competition between lattice directed and nano-step directed modes. Ago et al. systematically investigated four kinds of A-plane surfaces with different step height and orientation.[72] They found these two modes can cooperate to build the unique curved networks of SWNTs, which especially happened at the edge of Al_2O_3 with a large mis-cut angle. Moreover, the reason why some certain surface structures can direct the growing SWNTs has remained an open question so far. Jeong et al. performed the first-principles total-energy calculations and found that the SWNT alignment on sapphire attributed to the formed covalent bond between Al and C atoms.[73] Comparatively, Zhou C.W. supposed the topmost layer of oxygen atoms played the crucial role for sapphire,[74] and the alignment of SWNTs strongly correlated with their diameters.

3.3. External Field Directed Growth Mode

Interestingly, external fields, such as the electric and magnetic fields,[47,75] besides the inherent CVD parameters, can be introduced to be additional driving forces and to facilitate the preparation of aligned SWNTs, As we know, SWNTs seem like conducting molecular nanowires due to their unique electrical property. The applied field can validate the distinct dipole moment of SWNT, and the polarizability along its axis is greatly higher than that along its radial direction. In this way, the corresponding force can be applied to rotate and align the SWNTs as shown in Figure 4g. Dai et al. firstly demonstrated the electric-field directed growth of SWNTs.[47] It was found that the suspended SWNTs crossed the elevated poly-Si structures (Figure 4h). Especially, this method worked well when electric field was perpendicular to gas flow, which evidently excluded the gas flow effect. Furthermore, J. Zhang's group realized the enrichment of metallic nanotubes in electric field-assisted CVD systems as shown in Section 7. Although the original mechanism is unclear, magnetic field has already been utilized to direct the growth orientation of SWNTs.[75] Specifically, the alignment of SWNTs was well parallel to the applied magnetic field.

Comparing three exploited growth modes, it is obvious that the introducing of external fields demands complex apparatus with a high-cost. The gas flow directed mode takes the unique advantages to produce ultra-long SWNTs, while it severely

relies on a stable laminar flow, which is affected by the temperature, flow rate and location of substrate. Finally, the surface directed growth mode enables the facile, scalable and convenient preparation of aligned SWNT arrays with high density, especially on quartz substrates. Notably, the obtained SWNTs on these insulating surfaces are quite unsuited for the fabrication of bottom-gated nanodevices or integrated circuits. In this regard, many smart strategies have been exploited to transfer the grown SWNTs onto Si wafers, including the PMMA-mediated printing[76] and thermal release tape-based method.[77] It is a great challenge to maintain the alignment of CNTs and completely remove the residuals during the transfer process.

3.4. Construction of Complex Architectures

SWNTs with controlled geometries have attracted much attention in nanoelectronics and optoelectronics. The CVD growth process combines with various influential factors, some of which can jointly affect the geometries of prepared SWNTs. Following the synergistic effect of different directed modes, aligned SWNTs can form plenty of complex architectures, including serpentine SWNTs (**Figure 5**a),[78] cross-bar SWNTs (Figure 5b and c)[55,66] and SWNTs with specific turning angles (Figure 5d).[79,80] Serpentine SWNT[56] results from the spontaneous self-organization by crinkling individual ultra-long one

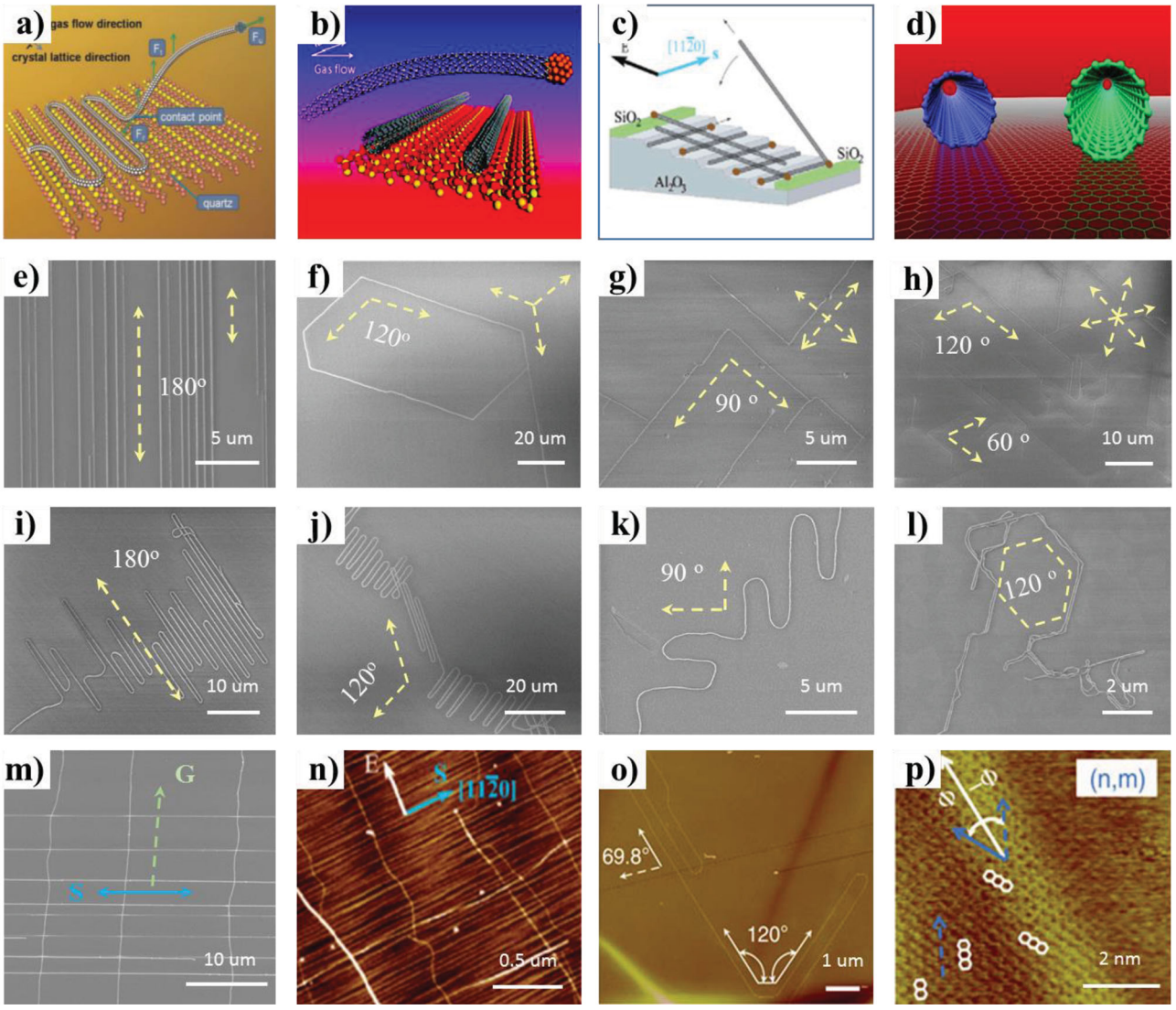

Figure 5. Construction of complex architectures by combining different directed growth modes. a-d) are the schematic illustrations of serpentine SWNT on quartz, cross-bar SWNTs in one CVD batch, cross-bar SWNTs by electric field and surface directed modes, and chirality dependent alignment of SWNT on graphene, respectively. (a) is reproduced with permission.[78] Copyright 2009, Wiley-VCH. e–h) are the scanning electron microscope (SEM) images of aligned SWNTs on ST-cut quartz, quartz (001), MgO (001), and mica, respectively. i-l) are the typical images of serpentine SWNTs on ST-cut quartz, quartz (001), MgO (001), and mica, respectively. (e–l) are reproduced with permission.[79] Copyright 2012, Elsevier. m, n) are the cross-bar SWNTs by combining gas flow-lattice and electric field-facet directed modes, respectively. (b) and (m) are reproduced with permission.[66] Copyright 2009, American Chemical Society. (c) and (n) are reproduced with permission.[55] Copyright 2006, American Chemical Society. o, p) are the AFM and STM images of SWNTs on graphite surfaces, respectively. (d), (o) and (p) are reproduced with permission.[80] Copyright 2013, American Chemical Society.

(Figure 5e) into many straight and parallel segments (Figure 5i), which can be achieved by combining the gas flow and surface directed growth modes. In this case, two key forces compete to determine the length of parallel segments and space of serpentine shape, which are the lattice–alignment force from substrate and shear friction force from the gas flow. During the landing process onto crystal surface, ultra-long SWNTs occasionally change its direction to follow the surface lattice because of the lattice–alignment force. We found that the gentle decrease of temperature and stable laminar flow can significantly improve the parallel length and reduce the spaces between parallel segments.[78] Moreover, the detailed analysis of AFM images indicated that the spaces also increased with the SWNT's diameters, which was exactly consistent with higher mechanical stiffness of larger SWNTs.[56] Accordingly, it is supposed that the electric field, replacing the gas flow, may work well to produce serpentine SWNTs on crystal surfaces. To the best of our knowledge, there is still a lack of related reports.

As we know, the interfacial interactions between SWNT and underlying substrate play a key role in its growth direction. On the basis of fundamental crystallography, there are five kinds of symmetries for all crystal materials, i.e., 1-, 2-, 3-, 4- and 6-fold. Besides the popular used quartz and sapphire substrates with 2-fold symmetry, we systematically studied the SWNT growth using quartz (001), MgO (001) and layered mica as substrates with 3-, 4- and 6- fold symmetry, respectively.[77] Interestingly, the obtained SWNTs also presented the homologous turning angles of 120°, 90° and 60° due to their anisotropic interactions as shown in Figures 5f and h. Analogous to ST-cut quartz, serpentine SWNTs along the corresponding three, four and six directions were also prepared by combining two directed modes as shown in Figures 5j, k and l, respectively. Interestingly, the aligned SWNTs can shape into closed loops due to the special angles, like 'T' and 'V'.

In addition, cross-bar SWNTs mean the orthogonal architectures of aligned SWNTs from different directed modes. Nowadays, three synergistic effects have been artfully designed to construct the cross-bar SWNTs: gas flow-gas flow, gas flow- lattice and electric field-lattice. Firstly, the cross-bar structures can be conveniently prepared through twice the gas flow directed growth process, and importantly the patterned catalyst strips should be perpendicular to each other.[44] Secondly, J. Zhang's group constructed the cross-bar SWNTs on quartz in one CVD batch by the gas flow and lattice directed modes (Figure 5m). This method indicated that the lattice directed SWNT was accomplished in advance, and then the ultra-long SWNTs directed by the gas flow fell onto its surface.[66] Finally, an electrical field can take the place of a gas flow to produce ultra-long SWNTs. The typical AFM image was shown in Figure 5n.[55]

Among all above methods, the obtained SWNTs along each direction are a mixture of different chiral structures. Graphene, an allotrope of carbon, refers to a monolayer of tightly packed atoms with two-dimensional honeycomb lattice.[81] The van der Waals interactions between different graphene layers are strongest when their configurations are AB stacking. Similarly, this equilibrium configuration can be achieved to the interface between SWNT and graphene. In this way, we demonstrated the chirality dependent alignment of SWNTs on a graphite surface (Figure 5d).[80] AFM results in Figure 5o revealed that the serpentine SWNT was produced along two directions due to the D_{6h} symmetry of graphene. Also, the angles between SWNTs and etched graphene trenches were arbitrary, like 69.8°. Furthermore, scanning tunneling microscopy (STM) characterization was performed to investigate their interfacial structures. The atomically resolved image clearly showed that there is chirality-selectivity in the alignment of SWNTs on graphene (Figure 5p).

4. Length Control

It is known that SWNTs have a high degree of aspect ratio, with up to macro-scale length along the axial direction while only nanometer scale of diameter. The length of individual SWNT along its axis can be measured directly using SEM with different voltage contrast[82] or optical microscopes with it decorated with nanoparticles.[83] It is proved that the unique properties of SWNTs, such as thermal conductivity,[84,85] electronic transport properties,[86] are related to their length. Besides, in order to meet the requirements of some applications, SWNTs with certain lengths are in need.[87–89] As far as it is concerned, SWNTs with certain lengths can be obtained by two approaches. One is through top-down strategy. Through the post-treatment process, SWNTs with different lengths can be cut into SWNTs with a uniform length. There are many post-treatment methods to achieve SWNTs with uniform lengths, such as mechanical force[44,90–92] or chemical reaction.[93,94] The other method is based on bottom-up strategy, which means that SWNTs with a certain length are selectively grown.[26,95,96] However, the top-down approaches often introduce some impurities, defects and even functional groups on the surface of SWNTs, which do great damage to the original properties of SWNTs. In the following part, we will first review the growth of ultra-long SWNTs, which could be used to further produce SWNTs with a uniform length through top-down methods. Then, the direct growth of SWNTs with a certain length using a nano-barrier will be introduced.

4.1. Synthesis of Ultralong SWNTs

Gas-flow-directed CVD is one of the most effective method to prepare SWNTs arrays with ultra-long length[44,96–99] (**Figure 6**). It is well known that the route of gas-flow-directed growth process follows kite-mechanism,[51] where catalysts lodge on the top of the as-grown SWNTs with successively dissolving and precipitating carbon atoms. With the floating grow process, the catalysts have more opportunities to contact with carbon sources to grow SWNTs, which benefit for the high growth rate of SWNTs and lead to the growth of ultra-long SWNTs. In 2002, with well-defined patterned catalyst nanoparticles, Dai et al. got 0.6 mm SWNTs at a growth speed more than 1 μm/s (Figure 6a).[99] Then, in 2004, Liu et al. reported a "fast-heating" process, which produced ultra-long SWNTs (Figure 6b) at a rate of 3 μm/s in a CO/H_2 system and 20 μm/s in a CH_4/H_2 system.[44,51] In the same year, Zhu et al. grew 4-cm-long SWNT (Figure 6c) at a grown rate of 11 μm/s using ethanol as

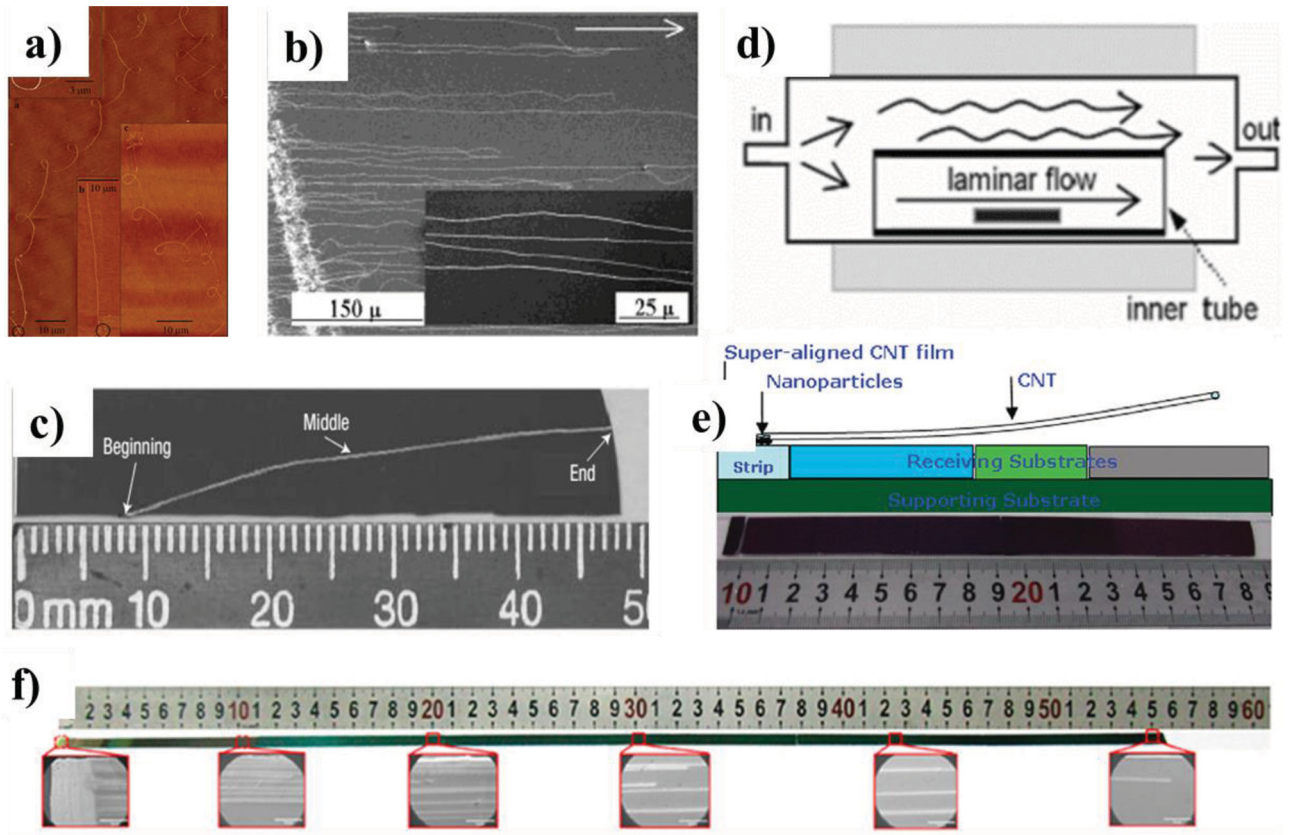

Figure 6. The length of ultra-long CNTs evolves with time. a) SWNTs grown with well-defined patterned catalyst nanoparticles. Reproduced with permission.[99] Copyright 2011, Elsevier. b) Ultra-long CNTs grown with "fast-heating" process. Reproduced with permission.[44,51] Copyright 2003, Wiley-VCH and Copyright 2004, American Chemical Society. c) 4-cm-long SWNTs grown with ethanol as the carbon source. Reproduced with permission.[60] Copyright 2004, Nature Publishing Group. d) 10-cm-long SWNTs grown with more stable laminar flow. Reproduced with permission.[97] Copyright 2005, American Chemical Society. e) 18.5-cm-long SWNTs grown with a super-aligned CNT film to support the catalysts. Reproduced with permission.[98] Copyright 2009, American Chemical Society. f) 55-cm-long CNTs grown with furnace-moving method. Reproduced with permission.[96] Copyright 2013, American Chemical Society.

the carbon source.[60] In 2005, with more stable laminar flow to stabilize the catalysts at the tip of growing SWNTs (Figure 6d), Kwang et al. grew 10 cm SWNTs with about 9 μm/s growth speed.[97] In 2009, by using a super-aligned SWNT film to support the catalysts, 18.5-cm-long SWNTs has been synthesized at a growth rate up to 40 μm/s (Figure 6e).[98] In 2010, Wei et al. achieved even higher growth rate of 90 μm/s and prepared 20-cm long few-walled CNTs by introducing trace of H_2O.[57]

Obviously, many factors can affect the growth rate and the maximum length of the produced long SWNTs. It is important to understand the dependence of the length on various parameters. Recently, Wei et al. analyzed the length distribution of horizontal ultra-long CNT arrays and the catalysts activity/deactivation probability. They found that the relative ratios of CNTs with different lengths[96] could be described by Schulz-Flory distribution, which is a mathematical function that usually be used to describe the relative ratios of liner condensation polymers of different length. The catalyst active life is the most important factor determining the length of CNTs. In order to keep the catalyst activity as long as possible during the growth of CNTs, Wei et al. have explored the optimal operation parameter, and prepared 55-cm-long CNTs (Figure 6f) at a growth rate of 5 mm/min.[96]

4.2. Synthesis of SWNTs with a Certain Length

The active growth time and growth rate of SWNTs depend on the activity and lifetime of the catalyst. However, it is difficult to stabilize all the catalyst nanoparticles at the same activity level; in another word, it is hard to make all SWNTs the same length at one synthesis process. To selectively grow SWNT arrays with certain length, one easy way is confining the spatial termination position of growing SWNTs, which means to obstruct the growth of SWNTs by instantaneously stopping the catalysts' activity possibility with additional barriers at a certain position. Firstly, taken the gas-flow-directed growth mode into consideration, ultra-long SWNTs are floating upon substrates, it will inevitably influence the gas flow and the growth of SWNTs if a barrier is put downstream to confine the growing SWNTs, whose height need to be higher than the flying height of SWNTs. Besides, if the grown SWNTs abided by surface directed growth mode, the SWNTs will grow along the specific

direction on the substrate surface. It can be understood that any sags and crests occurred on the single crystal substrate surface will affect the alignment of SWNTs. Taken in these senses, a convenient way to control the lengths of as-grown SWNTs is to fabricate an obstacle on the single crystal substrate surface to block growing SWNTs. The most typical example is to predefine the separation distance of catalyst lines to grow SWNT arrays on quartz substrate (**Figure 7**a and b), so the catalyst line can catalyze growth of SWNTs and simultaneously be barriers to limit the growing SWNTs across them.[71,100] Similarly, Rogers et al. introduced a layer of amorphous SiO_2 onto quartz surface, and SWNTs terminated at the edge of the SiO_2 layer because of the surface relief.[100] We have studied the lattice-directed grown SWNTs on quartz substrates terminated with ultra-long SWNTs as barriers[95] (Figure 7c and d). Firstly, SWNT nano-barriers were grown on a quartz substrate by the gas-flow-directed mode, and then lattice-directed SWNTs were grown. Since the gas-flow-directed grown SWNTs generally have a lager diameter than the lattice-directed grown SWNTs, the first grown SWNTs can act as natural barriers to obstacle the lattice-directed SWNTs to cross over. Our results showed that the lattice-directed grown SWNTs terminated when reached the SWNTs nano-barriers on the quartz substrate.

5. Density Control

Toward the fabrication of highly integrated circuits, well-aligned SWNT arrays with high density are highly desired. As mentioned in Section 3, the scientists of IBM research center have claimed that the desired horizontal SWNT arrays should have a density of 125 nanotubes/μm. There are several kinds of high density SWNTs, including vertically aligned SWNTs,[43,101] random SWNT film,[102–105] horizontal SWNT arrays,[50,106–108] and so on. This section will mainly focus on the horizontal SWNT arrays on substrates.

5.1. Growth of High Density SWNT Arrays

To achieve high-density horizontal SWNT arrays, scientists have developed lattice- or step-directed growth methods of SWNTs.[49,50] As we know, catalyst nanoparticles are the most important factor in the growth of SWNTs. Since SWNTs are grown from catalyst particles, SWNT arrays with ultra-high density could be obtained if there are high density catalyst nanoparticles and all of them could catalyze the growth of SWNTs. Unfortunately, not all the catalyst particles are active in the growth of aligned SWNTs. Thus, to improve the percentage of active catalyst nanoparticles are of high importance for the growth of high density SWNT arrays.

Liu and co-workers have produced high-density and perfectly aligned SWNT arrays on an ST-cut quartz substrate using patterned copper as a catalyst and ethanol as the carbon source (**Figure 8**).[71] As shown in Figure 8d, the density could be more than 50 SWNTs/μm. However, the reason why it could reach so a high density is still not clear. They supposed that much H_2O vapor can be obtained by dissociation of ethanol at high temperature, which made copper nanoparticles to keep high catalytic activity.[101,109] In their further study, a dense array of parallel SWNTs with densities of 20–40 SWNTs/μm on Y-cut quartz surface were synthesized by a multiple-cycle CVD method (Figure 8e).[110] The carbon source was stopped for several minutes intermittently in the growth process of SWNTs. New SWNTs were found to grow in the new CVD process. It means at least a part of catalyst particles could keep their catalytic activities after a CVD process. And they confirmed that more catalyst particles could be activated during the multiple CVD cycles. Rogers and co-workers reported another multiple CVD growth of SWNT arrays with high density.[111] As shown in **Figure 9**a, iron catalyst lines were firstly patterned on an ST-cut quartz substrate. After one ethanol CVD growth, SWNT arrays were grown in a direction orthogonal to the catalyst lines (Figure 9b). Then a narrow line SWNTs were removed by patterned oxygen

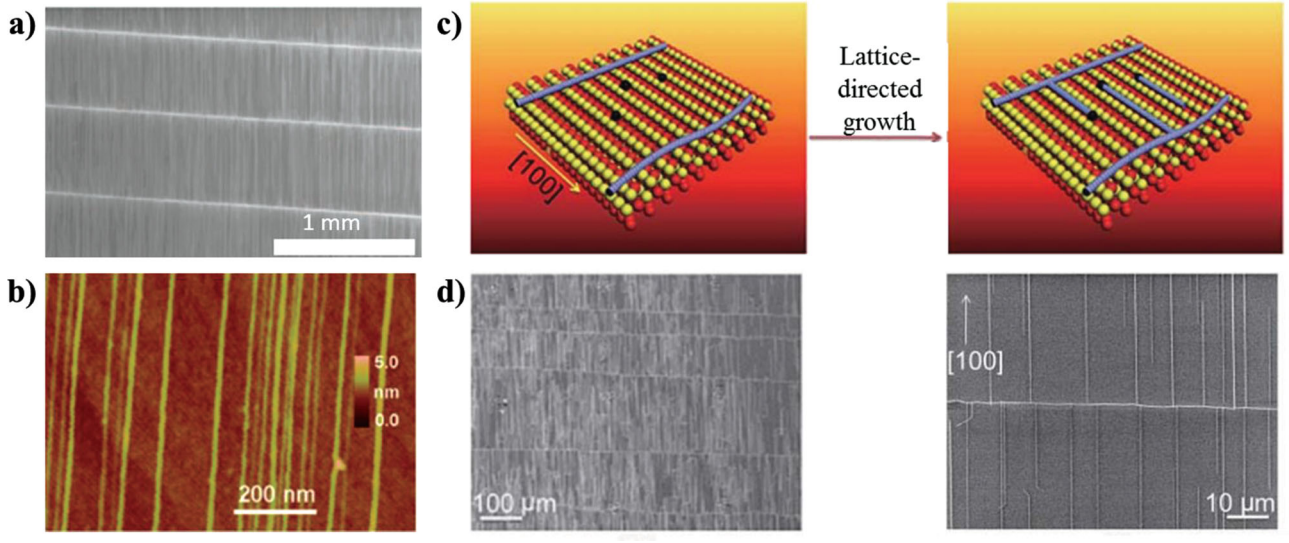

Figure 7. a, b) SEM and AFM images of high-density and perfectly aligned arrays of long SWNTs on quartz substrate. Reproduced with permission.[90] Copyright 2003, American Chemical Society. The bright stripes correspond to catalyst lines. c, d) Schematic illustration of nano-barriers-terminated growth of SWNTs on quartz substrate and typical SEM images. Reproduced with permission.[95] Copyright 2009, Springer.

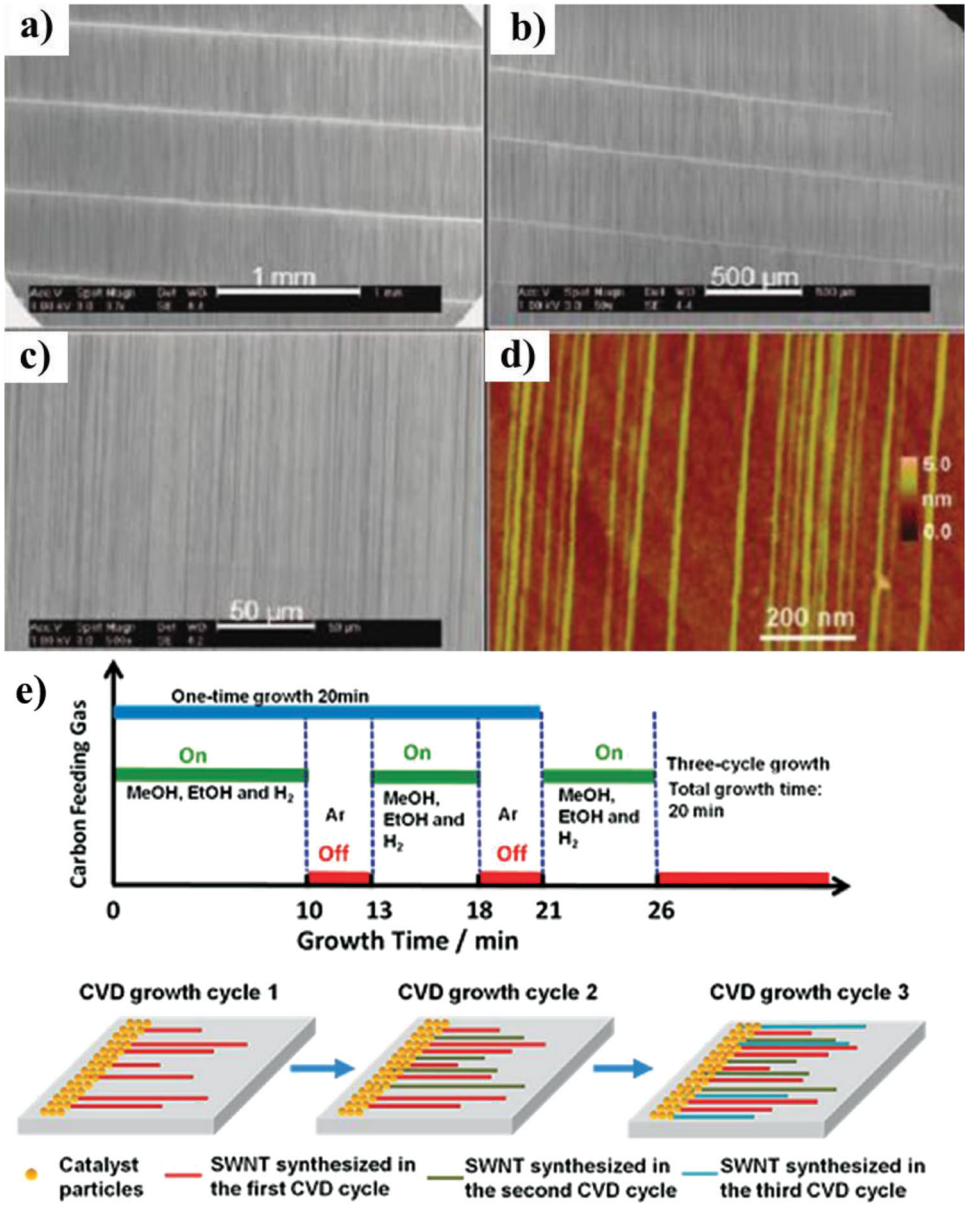

Figure 8. a, b) SEM images of high-density SWNT arrays on the ST-cut quartz substrate using patterned copper catalyst. c) High-magnification SEM image of the SWNT arrays. d) AFM image of high-density SWNT arrays. (a-d) are reproduced with permission.[71] Copyright 2008, American Chemical Society. e) Schematic illustration of growing high-density SWNT arrays by three-cycle CVD growth. Reproduced with permission.[110] Copyright 2011, American Chemical Society.

plasma (Figure 9c). After depositing new iron catalyst lines in the region (Figure 9d), a second ethanol CVD growth was performed and new SWNT arrays were obtained (Figure 9e). The conditions for the second growth should be carefully selected to protect pre-existing SWNT arrays from being damaged in the process of annealing and reducing the catalyst. In this way, the density could reach about 20–30 SWNTs/μm uniformly over the entire growth area and could be ~45 SWNTs/μm in some regions. The above methods to improve the density of SWNTs are all base on the treatment of catalyst particles. The first one keeps the copper catalyst activity. The second method is multiple-cycle CVD growth, which make catalyst nanoparticles have more chance to nucleate SWNTs. The third method is adding in new catalysts to grow new SWNTs.

For SWNTs growing on sapphire substrates, Ago and coworkers have achieved SWNT arrays with controllable density using Fe-Mo nanoparticles as catalysts. The density of their produced SWNTs could reach >20/μm^2.[112] They have also studied catalytic activities of single and binary metal catalysts for SWNT arrays growth on sapphire. And different density SWNT arrays could be achieved with varied CH_4 concentrations.[113] In principle, SWNT arrays with even higher density may be obtained by combining the advantages of the above methods.

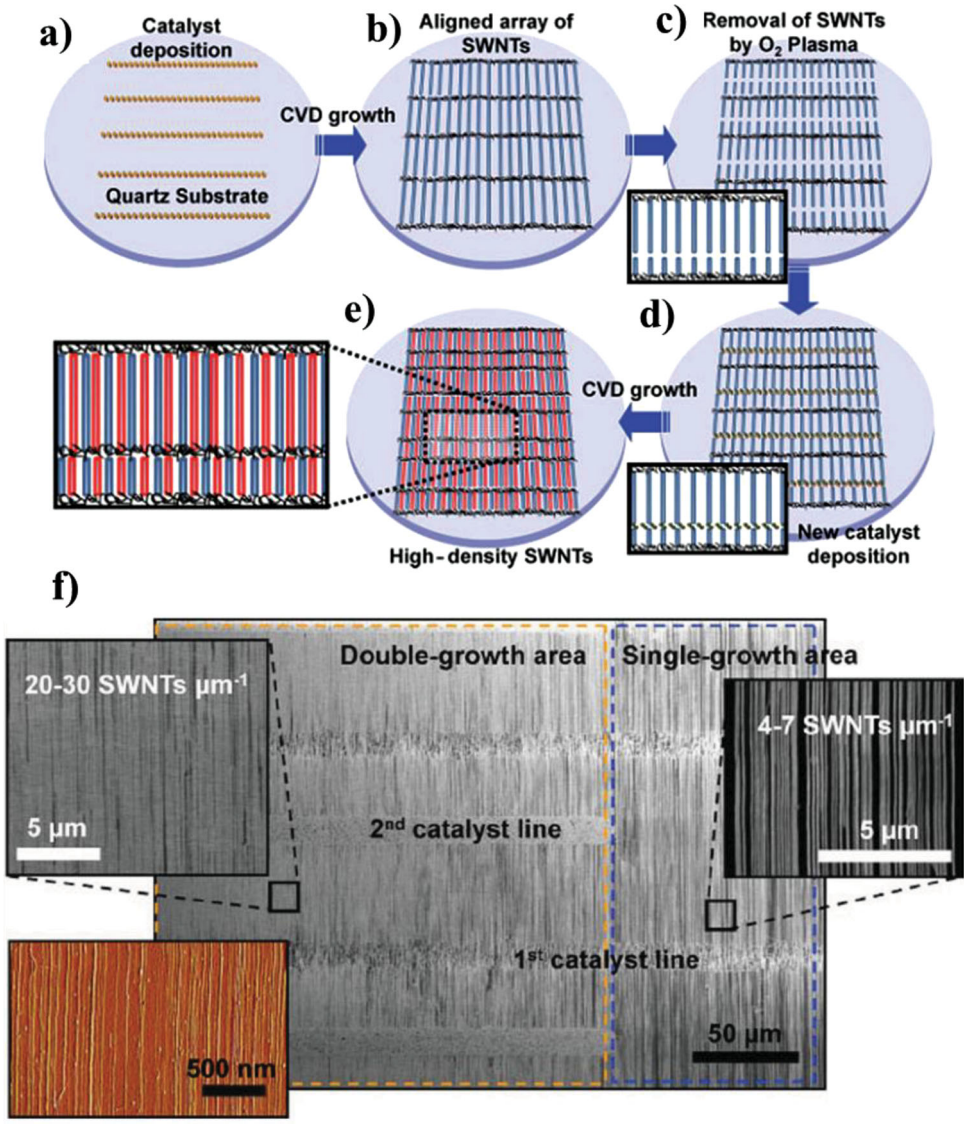

Figure 9. a-e) Schematic illustration of growing high-density SWNT arrays by multiple CVD cycles. f) SEM and AFM images of single and double growths of SWNTs on quartz substrate. (a–f) are reproduced with permission.[111] Copyright 2010, Wiley-VCH.

5.2. Multiple Transfer Process for High Density SWNT Arrays

Zhou's group developed a post-treatment method to prepare high density SWNT arrays.[114] Firstly, they have grew SWNT arrays with density 15–20 SWNTs/μm throughout the quartz sample using LPCVD technique. And then as shown in **Figure 10**, a stacked multiple transfer technique was developed to transfer the SWNT arrays from multiple starting quartz samples to one Si/SiO_2 substrate or many other target substrates, which could multiply the density of SWNT arrays. In theory, it could be repeated many times and thus obtains extremely high-density SWNT arrays. However, it would be difficult to keep the well alignment of SWNT arrays every time. They could repeatedly operate the same multiple transfer technique up to four times without any problem and achieve SWNT arrays with 55 SWNTs/μm after four time transfer. In fact, the SWNTs after transfer are not as straight as before, which could lead to increased tube-to-tube interactions, and limit the performance of SWNT nanodevices.

6. Diameter Control

Electronic properties of SWNTs highly depend on the structure of the SWNTs, including the diameter and the chirality. Therefore, for many applications, especially for nanoelectronics, the selective growth of SWNTs with certain diameters and chiralities is very important. Among the conditions in CVD system, catalyst, temperature and gases are the most important factors determining the diameters of the SWNTs. In this part, the relationship between the size of catalysts and the diameters of SWNTs will be reviewed, and then, the effect

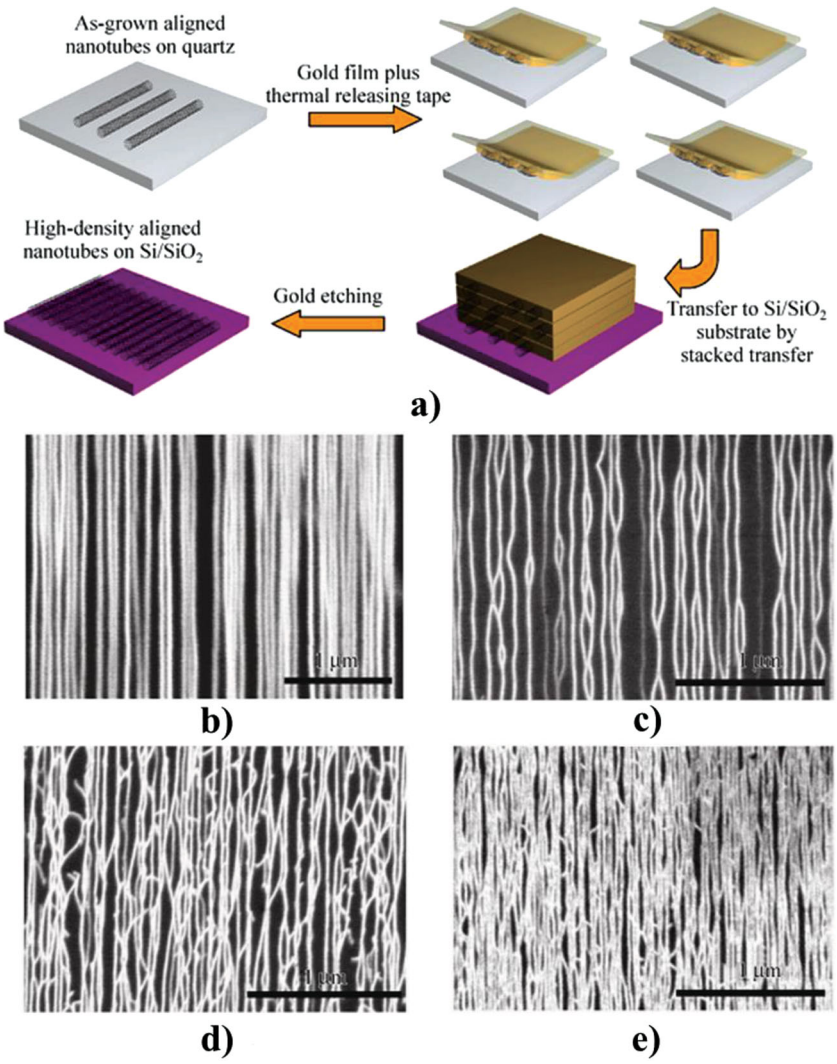

Figure 10. a) Schematic illustration of using stacked multiple transfer process to further increase the SWNT arrays density. b) SEM image of the as-grown SWNT arrays on quartz substrate with a density of 15 SWNTs/μm. c-e) SEM images of SWNT arrays transferred to Si/SiO_2 substrates with one-time, two-time, and four-time transfer, respectively. The corresponding average densities are 15, 29, and 55 SWNTs/μm. (a–e) are reproduced with permission.[114] Copyright 2010, Springer.

of temperature and gases will be reviewed as well. Based on the understanding of the mechanisms governing the diameters, SWNTs with specific diameters might be selectively prepared.

6.1. Dependence of Diameter on Catalysts

The diameters of SWNTs directly depend on the diameter of catalysts,[115] as proved by the observation.[115–118] Dai's group[119] proved the positive correlation between catalyst diameter and SWNT diameter. As shown in **Figure 11**a, they use iron-storage protein, ferritin, to synthesis discrete catalyst with tunable diameters.

The ferritins contained different amounts of iron atoms were stabilized against agglomeration in aqueous solutions because of functional groups on the proteins, and would be isolated when deposited on substrates. The organic shell was removed on the high temperature and mono-disperse oxidized iron core was got. Then the discrete nanoparticles were used as a catalyst to produce SWNTs by CVD, and the diameters of SWNTs were characterized. They found that the diameter of SWNT was slightly smaller than that of a catalyst. By in situ TEM, the growth of SWNTs from the isolated catalysts and catalyst nanoparticles was directly observed. Because the sizes of the metal nanoparticles are difficult to control, the produced SWNTs typically exhibit a large diameter distribution from 1 to 5 nm.[120] To realize a better control of the diameters of catalysts, Itami and co-workers used well-defined carbon nanorings as templates.[121] [N]cycloparaphenylenes ([n]CPPs) are a series of molecules that have different diameters depend on the number [n]. Two kinds of CPPs were mainly reported in their work, which are [9]CPP and [12]CPP. The diameter of [9]CPP is 1.2 nm, while that of [12]CCP is 1.7 nm. As shown in Figure 11b, the diameters of SWNTs have a narrow range, and the distributions are different between different catalysts. When using [12]CCP as catalysts, most of the SWNTs were distributed in the diameter range of 1.3–1.7 nm, which is close to that of [12]CPP. Many methods to prepare uniform catalysts have been developed. Lieber et al.[122] used $Fe(CO)_5$ as the reactant and oleic (lauric and octanoic) acid as the capping ligand to yield iron cluster solutions with distinct and nearly mono-disperse diameters firstly, and then used these clusters as the catalysts on the oxidized silicon surfaces to grow SWNTs with ethylene or methane precursors. In their experiments, the SWNTs obtained from iron nanoclusters with average diameters of 3, 9 and 13 nm had diameters of 2.6 + 0.8, 7.3 + 2.2 and 11.7 + 3.2 nm, respectively. Besides, Liu et al.[123] used a series of molecular nanoclusters as catalyst which were synthesized by Muller and his coworkers.[124,125] The molecular nanoclusters are based on the molybdenum oxide which has the specific composition. In their experiment, they chose $\left[H_xP \subset Mo_{12}O_{40}H_4Mo^{VI}_{72}Fe^{III}_{30}(CH_3COO)_{15}O_{254}(H_2O)\right]\cdot 60H_2O$ as catalyst precursors and use 3-aminopropyltriethoxysilane (APTES) to modify the silicon dioxide to avoid the aggregation. They finally got a narrow range of diameter as they expected. Recently, J. Zhang's group reported a method for controlling the diameter of SWNTs by the SiO_2 nanoparticles.[32] Through the process shown in **Figure 12**a, SWNTs were grown with different range of diameters by depositing different layers of APTES on Si substrate (Figure 12b). Using these SiO_2 nanoparticles as nucleation centers, the final diameter distribution of nanotubes are correlated with that of SiO_2 nanoparticles.

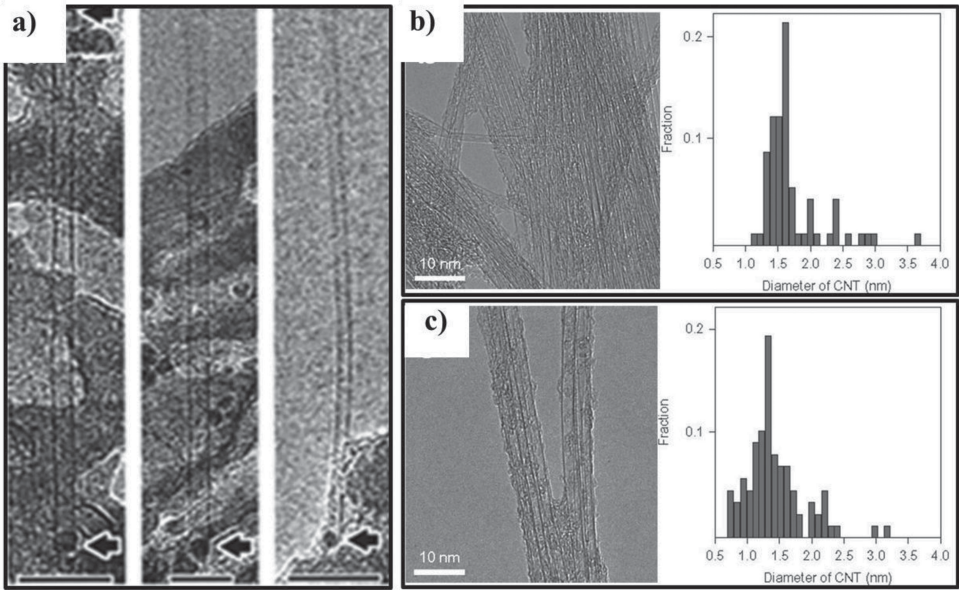

Figure 11. a) TEM images showing particle- SWNTs relationships. Dark dots at the bottom of the images are the discrete nanoparticles. Scale bars are 10 nm. Reproduced with permission.[119] Copyright 2001, American Chemical Society. b, c) TEM images and diameter distribution of SWNTs grown from [12]CPP (b) and [9]CPP (c). (b) and (c) are reproduced with permission.[121] Copyright 2013, Nature Publishing Group.

6.2. Dependence of Diameter of SWNTs on Temperature

Temperature is another major factor affecting the diameters of SWNTs. As mentioned in the above, the sizes of catalyst nanoparticles always play the most important role in determining the diameters of SWNTs. One effect of temperature is inducing the aggregation of catalyst. The higher growth temperature is, the faster diffusion of catalyst is at nanoscale. Because of the Ostwald Ripening, the small catalyst particles will become smaller and the bigger particles will

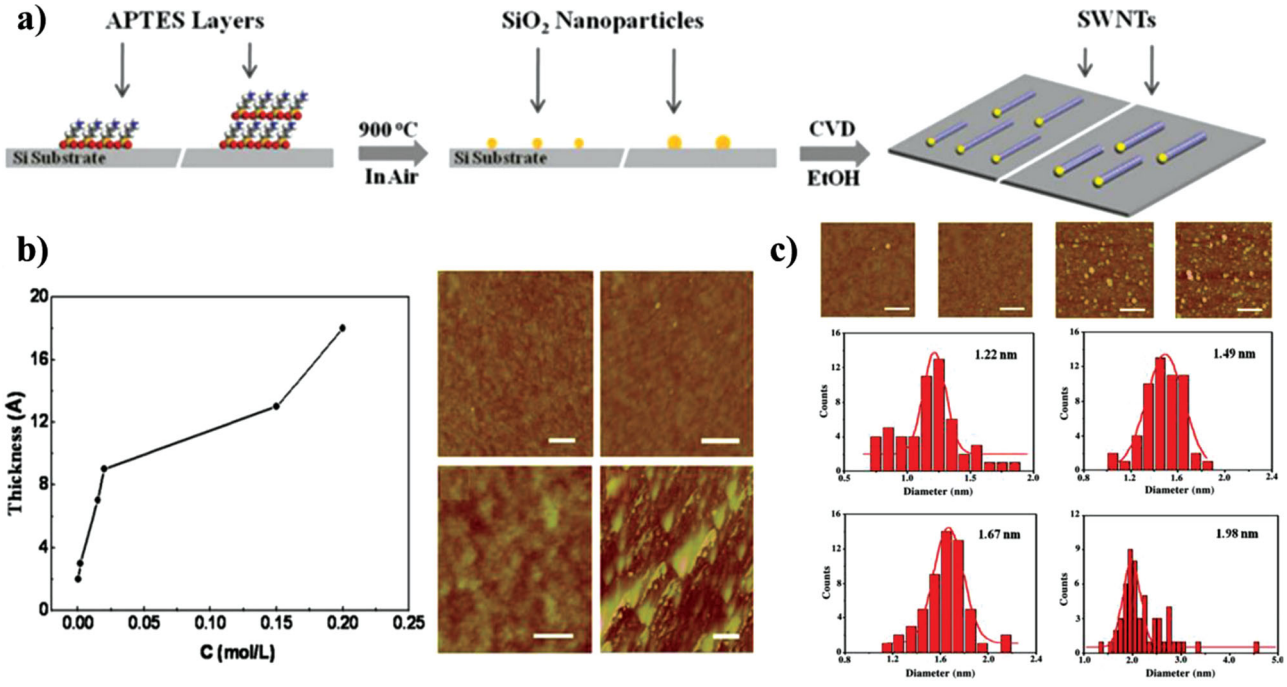

Figure 12. a) A diagram of diameter controlled growth of SWNTs from SiO_2 nanoparticles. b) Thickness variation of APTES layers as a function of solution concentrations. c) AFM images of assembled APTES layers when the concentration was 2.0×10^{-4}, 2.0×10^{-3}, 1.5×10^{-2} and 1.5×10^{-1} M, respectively. The scale bars are 0.25 μm. (a-c) are reproduced with permission.[32] Copyright 2011, Elsevier.

become bigger. According to this, different range of diameter of catalysts will appear at different temperature. At the same time, a certain amount of carbon resource will fit to some catalysts with proper diameter to grow SWNTs, while others will not. Catalysts with smaller diameter will be poisoned by the amorphous carbon, and some catalysts with bigger diameter cannot grow SWNTs due to the absence of enough carbon.[126] As a result, SWNTs with the same range of diameters to that of catalyst will be obtained. Generally, when the growth temperature becomes higher, the range of diameter distribution becomes bigger, and the diameter of SWNT will be bigger, too. Actually, the diameter of SWNT and temperature has more complicated relation. J. Zhang's group[127] reported that, the diameter of a SWNT could be controlled by changing temperature. **Figure 13** shows that an oscillation of the diameter of a SWNT will happen with varying temperature. Higher temperature led to thinner SWNTs while lower temperature led to thicker ones. Zhang et al. also believed that the diameter of SWNTs changes are highly correlated to their primary diameters. Also, there will be various probabilities of different diameter changes below a maximum, depending on the initial diameter. If the primary diameter is around 1.6 nm, the diameter will change the most, and the maximum diameter changes will be much lower for SWNTs with a larger or smaller diameter. Obviously, it indicates that the diameter modulated by temperature is limited. In addition, the relationship between the temperature and diameter was also calculated based on this model.

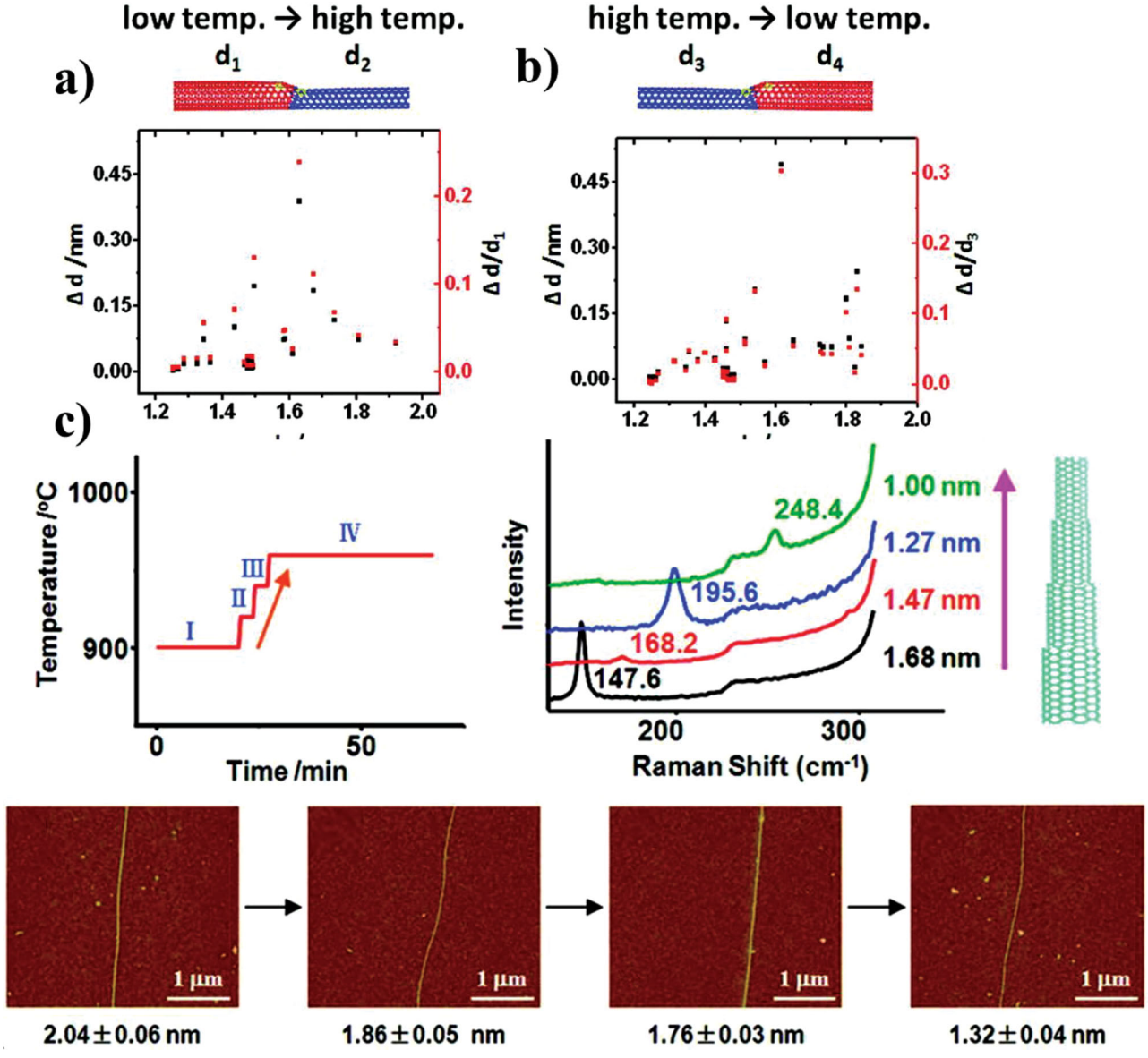

Figure 13. The relationship between the change of diameter (Δd) and the initial diameter: a) from low temperature to high temperature ($\Delta d = |d_2-d_1|$); b) from high temperature to low temperature ($\Delta d = |d_4-d_3|$). c) The ascending temperature-time curve and typical results of an ultra-long SWNT grown under the temperature-time process in panel. (a-c) are reproduced with permission.[127] Copyright 2003, American Chemical Society.

6.3. Dependence of the Diameters of SWNTs on Gas Feeds

Besides catalysts and temperature, gas feeds, such as different carbon resources, also have some effects on the diameter of SWNTs.[128–133] For example, the SWNTs produced from CH_4 have larger diameters and broader distributions than those obtained from CO, due to the introducing of hydrogen, a byproduct of the CH_4 decomposition reaction. Dai's group found that hydrogen existing in the gas has a dual effect on the nucleation of carbon, the formation of the SWNT's cap and the growth of the SWNT.[19] Except increasing the rate of reduction and sintering of metal clusters, hydrogen also prevents the nucleation of carbon species on the surface of catalysts by decreasing the carbon surface variation. As a result, the formation of the cap occurs at a larger size and the cap defines the diameter of SWNTs. Besides, changing the percentage of hydrogen in the gas also influence the diameter of SWNTs. Other gases, such as NH_3,[129] can play the similar role as hydrogen and have also been used to promote the production of large-diameter SWNTs with a narrow diameter distribution. It is proposed that small amounts of NH_3 could work as an etching agent to etch the nanotubes with smaller diameters due to their higher curvature, thus lead to a slightly enlarged average diameter of the produced nanotube. In contrast, Kauppinen et al.[134] argued the NH_3 etching action may affect on the catalyst clusters during nucleation, especially on the dangling bonds at the growing edge of the hexagonal network, suppressing the growth of smaller chiral angle tubes that have relatively more dangling bonds.

7. Semiconducting/Metallic Property Control

Generally, the as-produced SWNTs always contain both metallic (m-) and semiconducting (s-) ones, normally with a ratio of 1/2, which will dramatically decrease the performance of SWNT devices. For many applications, especially in electronics, the as-produced SWNTs must be separated into metallic and semiconducting before use. During the past decades, some separation approaches have been developed, including in situ growth and post-growth separation.

7.1. In Situ Growth of S-/M- SWNTs

For the in situ growth separation of s-/m- SWNTs, there are two typical approaches, which are a weak oxidative gas method and external field perturbation. The introduction of weak oxidative gas during the growth of SWNTs is proved to be an efficient way to preferentially grow s-SWNTs. In 2009, Liu et al. reported the selective growth of well-aligned s-SWNTs on quartz substrate using ethanol/methanol as the carbon feeds and copper as catalysts.[130] The percentage of s-SWNTs in the arrays was more than 95%, as determined by both Raman spectroscopy and electrical measurements. The ratio of s-SWNTs is about 2/3 when only ethanol was used as the carbon feeds,[35] indicating that the introduction of methanol is the key factor to the selective growth of s-SWNTs. However, only using methanol as carbon source even can not get SWNTs at 900 °C since the decomposition temperature of methanol is much higher. It was proposed that when using an ethanol/methanol mixture, the ethanol decomposed to grow SWNTs and the OH radical from methanol can selectively etch m-SWNTs because of their smaller ionization potential as compared to s-SWNTs.[131] They further studied the etching effect of water vapor for selective growth of enriched s-SWNTs.[132] The results showed that m-SWNTs were preferentially etched by water vapor under a certain condition.[133] Besides, they also showed that the ratio of carbon source to hydrogen also affected the ratio of s-/m- SWNTs. By optimizing the water concentration and gas, SWNT arrays with over 97% of s-SWNTs were obtained. Recently, they developed an improved multiple-cycle growth method including the treatment of SWNTs with water vapor after each growth cycle, and obtained high density s-SWNT arrays (~10 SWNTs/μm).[108] The introducing of weak oxidative gas during the process of growing SWNTs might be one of the most efficient methods to preferentially grow s-SWNTs.

Besides that gas feeding, other conditions might also influence the selectivity between m- and s- SWNTs. In 2004, Dai and coworkers reported the growth of 90% s-SWNTs by a PECVD system at 600 °C.[134] However, they did not explain the mechanism for the selectivity. In 2009, Zhang's group reported an in situ ultraviolet irradiation method to grow s-SWNT arrays,[135] which was shown in **Figure 14**(a, b). With the introduction of a UV beam into the CVD system, 95% s-SWNT arrays have been grow. Zhang et al. proposed that m-SWNT caps were destroyed at the

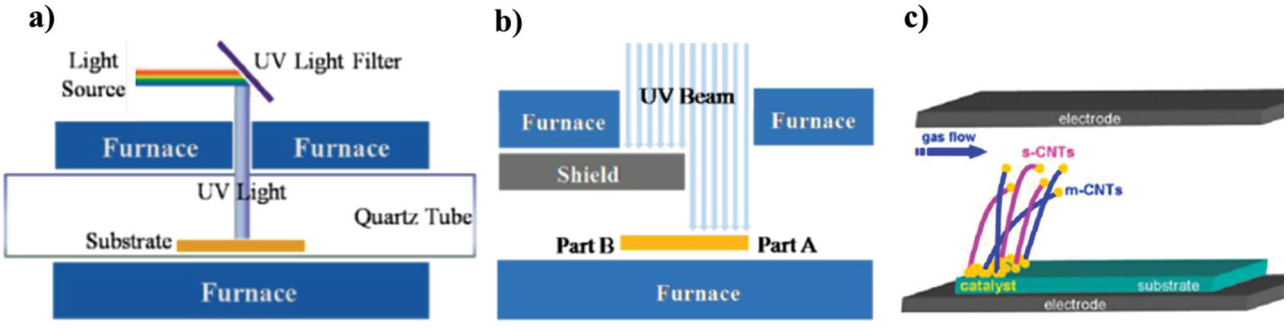

Figure 14. a) Sketch map of the homemade CVD system. b) Schematic illustration of the comparison experiment for SWNT growth with and without UV irradiation. (a) and (b) are reproduced with permission.[135] Copyright 2009, American Chemical Society. c) Illustration of the electric field effect on the growth of m-SWNTs. Reproduced with permission.[52] Copyright 2011, Elsevier.

very beginning of growth by UV irradiation through free radical reaction, while the s-SWNT cap survived and continued growing into s-SWNT arrays. In another work, an electric field-assisted CVD was developed to preferentially grow m-SWNTs (shown in Figure 14c) and the percentage of m-SWNTs could be 80%.[52] Those results show that the introduction of external fields would contribute to preferentially growth of s-/m- SWNT. However, the mechanism is still not very clear and needs more investigation.

7.2. Post Growth Separation of S-/M- SWNTs

Though separating SWNTs in the growth process is attractive, post growth separation of SWNTs is easier to realize. Many efforts have been made to separate metallic and semiconducting SWNTs,[136–152] although it is still far from satisfying the exciting application of SWNTs such as in all carbon electronic devices. Though separation in liquid phase has been well developed,[152–156] directly separation on the substrate surface is more compatibility with semiconductor industry. In this section, we will focus on the post growth separation of m-/s- SWNTs which are grown on surfaces.

According to the principle of the separating process, there are mainly five methods. The first one is electrical breakdown. As we know, the conductivity of m-SWNTs is greater than s-SWNTs, so m-SWNTs could be breakdown by the Joule heat resulted from big current with the s-SWNTs remaining on the surface.[157] Also based on this mechanism, Rogers et al.[158] coated SWNTs with a solid polymer layer and then applied an electrical voltage, which led to a large current flowing in the m-SWNTs, heating the polymers around them and finally leading to exposure of m-SWNTs, which thus could be selectively removed (**Figure 15**a). The second method is using gas to selectively remove the unwanted SWNTs at the surface. In 2003, Kwanyong et al. reported that carbon dioxide can selectively etch zigzag nanotube by using density functional calculations.[159] Besides, in 2006, Dai et al. demonstrated that a methane plasma followed by an annealing process could selectively hydrocarbonate m-SWNTs with s-SWNTs retained (Figure 15b).[160] Though most gas reactions remove m-SWNTs selectively, etching s-SWNTs is also possible. In 2009, Liu et al. reported that s-SWNTs could be selectively etched using SO_3 as etchant.[142] The third method is using electromagnetic radiation to selectively remove unwanted SWNTs. In 2004, Kenzo et al. proposed a laser resonance chirality selection method to remove SWNTs with specific chirality from mass of SWNTs by intense laser irradiation (Figure 15c).[161] The reason is when the van Hove singularities in the density of states of some SWNTs matches the energy of the incident photon, these SWNTs will be oxidized and are removed selectively. In 2008, Song et al. reported that they can use high-power microwave radiation in the infrared and radio frequency range of the electromagnetic spectrum to selectively removing m-SWNTs from s-SWNTs in a powder due to the fact that the dielectric constant of m-SWNTs is greater than s-SWNTs and will absorb more energy.[162] Expect the laser and microwave radiation, researchers also tried other forms of electromagnetic radiation to separate m/s-SWNTs. In 2008, Zhang's group reported that long-arc xenon-lamp irradiation can be used to prepare densely packed, well aligned individual s-SWNTs and the percentage of s-SWNTs is estimated to 95%.[138] The forth method makes use of the different response of m-SWNTs and s-SWNTs to mechanical stress, which is less reported. In 2010, Yang et al. showed that the electrical properties of armchair m-SWNTs are least sensitive to tensile strain, so when tensile strain is applied to suspended SWNTs on substrate, the resistance of armchair m-SWNTs nearly keep constant while that of other types of

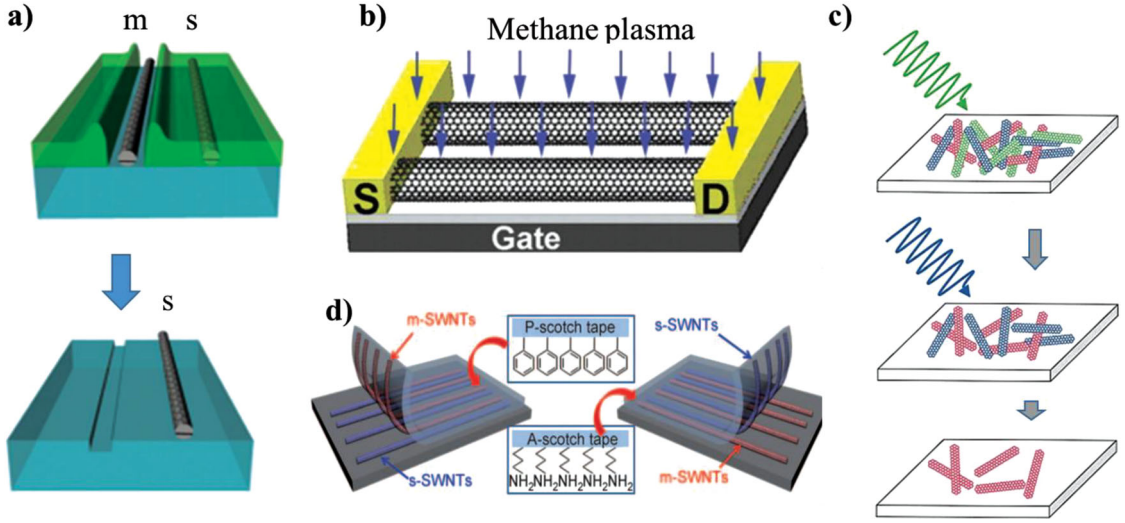

Figure 15. Post separation of metallic and semiconducting SWNTs on surfaces. a) Schematic illustration showing using Joule heating to induce thermal gradients that drive flow of thermo-capillary resist away from the m-SWNT to form open trenches around m-SWNTs and to selectively remove m-SWNTs. Reproduced with permission.[158] Copyright 2013, Nature Publishing Group. b) Schematic of the methane plasma treatment step to remove m-SWNTs with s-SWNTs retained. Reproduced with permission.[160] Copyright 2006, The American Association for the Advancement of Science. c) Schematic illustration showing to selectively remove SWNTs which are in resonance with the laser. Reproduced with permission.[161] Copyright 2004, AIP Publishing LLC. d) Schematic of SWNT separation using P- and A-scotch tapes to selectively remove m- and s-SWNTs respectively, on the sapphire substrates. Reproduced with permission.[156] Copyright 2011, Wiley-VCH.

SWNTs increase very much, leading to the selective burning off of armchair m-SWNTs. The fifth method is based on covalent selective interaction between SWNTs and other molecules. In 2011, Zhang group reported a "scotch tape" method.[156] Zhang et al. prepared P-scotch tape and A-scotch tape, which their surfaces were modified by phenyl functional groups and amine functional groups, respectively. Because phenyl functional groups have strong interaction with m-SWNT, P-scotch tape can selectively remove m-SWNT from SWNT arrays with the s-SWNTs remained. S-scotch tape has adverse behavior (Figure 15d). Furthermore, J. Zhang et al. proposed another procedure to separate m-/s-SWNT arrays on ST-cut quartz surface by washing off m-SWNTs using SDS aqueous,[163] which produced high quality horizontally aligned SWNT arrays with over 90% s-SWNTs.

8. Chirality Control

Chirality control is the ultimate target of structure controlled synthesis of SWNTs. Chirality of a SWNT determines its electron band structure, optical properties, and electric transport properties, which are the critical factor for many of its applications. The challenges of chiral control lie on the similarities in SWNT structure, the absence of characterization methods for chirality, and the limited understanding of growth mechanism. At present, the chiral controlled growth strategies could be divided into three groups based on different mechanism including: dependence of growth rate on the chirality of SWNTs, influence of catalyst and gas on the chirality, and control the chirality by cap engineering.

8.1. Dependence of Growth Rate on Chirality

SWNTs with different chirality have different growth rate, which could be used to control the chirality of SWNTs. Theoretical simulation[164,165] showed that a SWNT with a big chiral angle will grow much faster than those with a small one. Particularly, if a SWNT is armchair one whose chiral angle is 30°, it has more unsaturated bonds on the growing edge of the hexagonal network, and thus urgently needs to form a new bond to low its energy. Experimentally, Bandow S. et al.[166] found that chiral angles of SWNTs are all in the range of 20° to 30° at different temperatures. Moreover, Maruyama B. and his coworkers[167] used in situ Raman to track the growth process of SWNTs, and found a linear relationship between the chiral angle and growth rate, as shown in **Figure 16**a and b. Based on this fact, SWNTs with a specific range of chiral angles could be selectively obtained by extending the growth time thus to suppress the percentage of SWNTs with a low growth rate.

8.2. Dependence of Chirality of SWNTs on Catalyst and Gas

Catalyst played the most significant role in determining the structure of SWNTs. It shows that using binary alloy catalysts, changing the species of the catalyst and the state of catalyst during growth will contribute to the enrichment of chiral SWNTs. For example, catalysts with narrow distribution of diameter will lead to a narrow distribution of nanotube chirality, due to the direct relation between the chiral and diameter. According to this, Resasco's group[168] synthesized CoMoCAT catalysts and obtained SWNTs mainly composed of (6,5) and (7,5), shown in Figure 16c and 16d. They suggested that, in their method, Mo oxides exist and interact with Co to stabilize the Co catalyst against aggregation at the high-temperature. They also found that changing the Co:Mo ratio, the interactions will vary respectively. At the low ratios, a Co layer covers Mo oxide highly dispersed on the catalyst particles. When being exposed to CO, Co is reduced and migrates on the surface to form small metallic Co cluster which can grow SWNTs, because of the disruption of Mo layer with the Mo oxide converted into Mo carbide. And then, carbon deposits on the clusters, leading to the formation of relatively small diameter SWNTs. Similarly, Sankaran's group[169] prepared Ni:Fe catalyst nanoparticles with different Ni:Fe ratios for the growth of SWNTs. The results show that the Ni:Fe ratio can affect the SWNTs chirality. They explained it based on the specific structure of catalyst, such as exposed crystal face. It may be controversial since we cannot confirm the state of the catalyst, solid or liquid, under the growth conditions. As we know, the metal has a lower melting point at nanoscale than in block. In most cases, we believe it is in liquid and the growth of SWNTs follows the VLS mechanism. However, due to the limitations of experimental technique, in situ observation is still lacking at present to interpret the above chirality selective mechanism.

Besides catalysts, other factors also have an impact on chirality of SWNTs. For example, different carbon sources, CH_4 and CO,[170] will lead to different distribution of chirality. The main reason is considered to be selectively etching of the SWNTs by the by-products of carbon sources. He M.S. et al.[170] used TEM to explore the relationship between the chirality distribution and carbon sources. They found that CO contributes to the growth of SWNTs with big chiral angle, and CH_4 leads to random distribution, which are attributed to the preferred cap nucleation associated with the carbon feeding rate on the catalyst. Chen's group[171] got the similar result with He M.S., and they achieved the SWNTs mainly consist of (9, 4), (8, 4) and (8, 6). In addition, HiPco method was developed by Smalley's group,[115] and could be used to syntheses SWNTs mainly containing (7, 6) and (6, 5). In addition of carbon resources, other gases introduced into the system, such as NH_3,[129] have the similar effects. However, all the above investigations got SWNTs with some chiralities enriched. Breakthrough is needed to be made to prepare SWNTs with a single chirality.

8.3. Control Chirality of SWNTs by Cap Engineering

Cap engineering is a smart alternative strategy to control the chirality of SWNTs. The initial cap structures of SWNTs directly determine their sequent chiralities. Thus, it is possible to realize the controlled growth of nanotubes with certain chiralities by controlling the cap. However, it is not easy to finely control the structure of the cap in experiment. For this purpose, J. Zhang's group developed a SWNT growth method using opened C_{60} as a cap via an open-end mode.[172] Firstly,

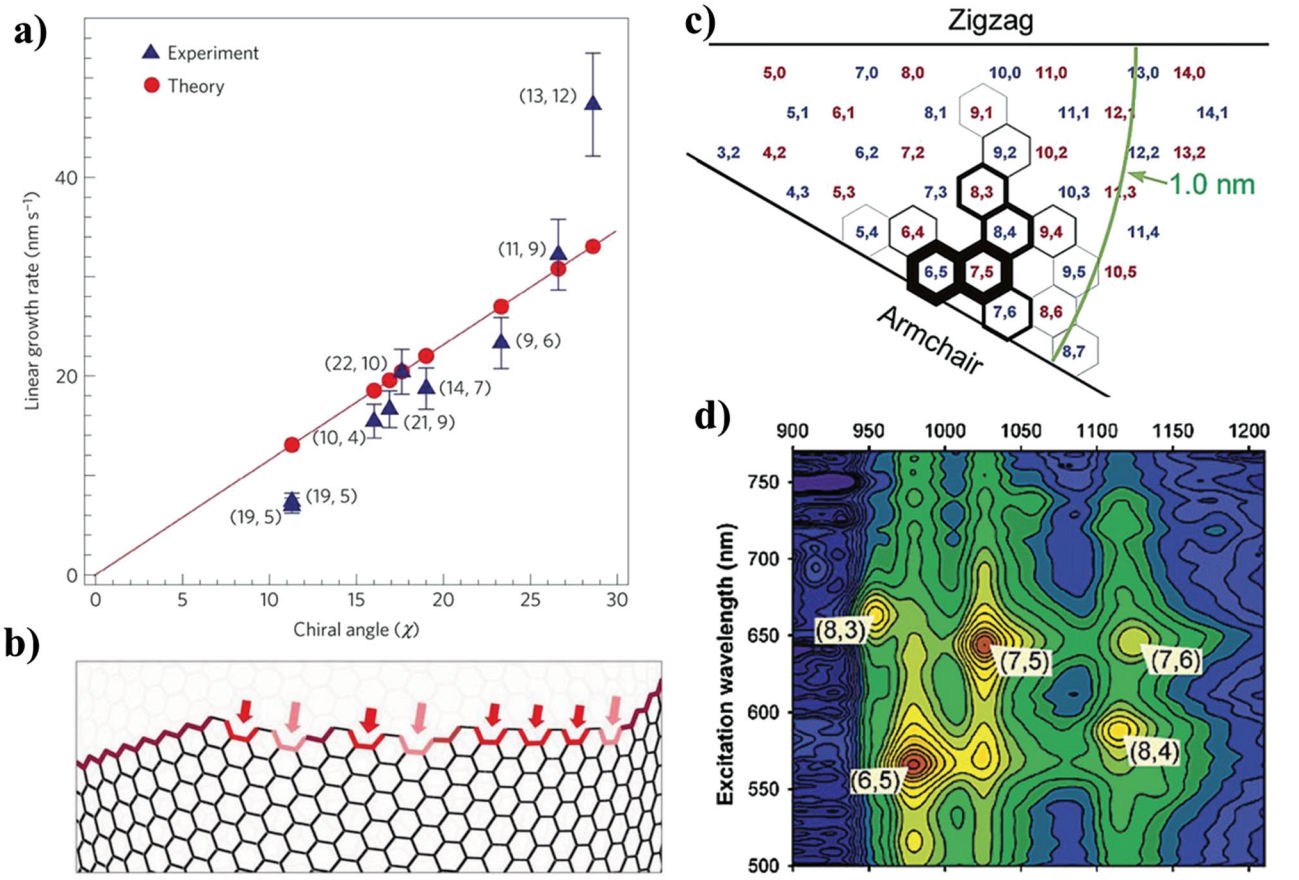

Figure 16. a) Chirality-dependent growth of SWNT. The linear growth rates (blue triangles) along with assigned (*n*,*m*) chiral indices are plotted against the chiral angle. b) A schematic of the structure of a SWNT edge. (a) and (b) are reproduced with permission.[167] Copyright 2012, Nature Publishing Group. c) (*n*,*m*)-resolved intensity map for the CoMoCAT sample. The thickness of each hexagonal cell in the graphene sheet is proportional to the observed intensity for that structure. Red and blue labels code for mod (*n*-*m*,3) families, and the arc indicates tube diameters of 1.0 nm. d) Contour plots of normalized fluorescence intensities for the CoMoCAT sample. (c) and (d) are reproduced with permission.[168] Copyright 2003, American Chemical Society.

fullerendione was thermally oxidized to open its carbon cage at different temperatures. Secondly, water vapor was used to mildly remove any possible amorphous carbon around the formed cap. Notably, the annealing process at high temperature was crucial to activate the cap, and it further affects the diameter distributions of the obtained SWNTs. Briefly, the higher the annealing temperature is, the smaller diameter of the grown SWNTs are. Moreover, the diameter displays a step distribution due to the instability of C_{60} at high temperature. Further, using the amplified growth method developed by Tour's growth,[173] Ren and his coworkers[174] proposed the concept of "Cloning carbon", that is, using SWNTs as the "cap" for further growth to get SWNTs with the same chirality. In 2009, J. Zhang's group[92] reported the successful "cloning" of SWNTs, as shown in **Figure 17**a. By using short SWNTs cut by oxygen plasma as "seeds/catalysts", "new/duplicate" SWNTs have been elongated from the parent segments with the remained chirality. It is found to be important to open and active the end of the seeds, which is fully proved by AFM and Raman spectroscopy. However, the growth efficiency is relatively low. Recently, Zhou and Zheng[175] enhanced the grow efficiency by combing liquid phase separation and VPE, as shown in Figure 17b. The seeds for cloning were carbon nanorings, which were synthesized by liquid phase with a high purity. The basic principle of these methods is based on the Diels-Alder reaction. Without this principle, J. M. Tour and his coworkers[173] have achieved this goal through reloading the catalyst at the end of SWNTs to promote the continued growth of SWNTs, such as in Figure 17c.

Although several strategies have been exploited to control the chiralities of the as-grown SWNTs, a breakthrough is still need to be made to realize the high efficiency control of chirality which is suitable for large scale production.

9. Chirality Identification of SWNTs

Chiral structure (chiral angle, handedness and chiral index) identification of SWNTs is the prerequisite for their fundamental researches and many promising applications. Although an enormous progress is made on the CVD controlled synthesis,[106] the accurate and convenient approach is lack to identify the chiralities of obtained SWNTs, owing to the nanometer size and diverse structures.[176,177] AFM is widely used to estimate SWNT's diameter. However, the measured diameter of SWNT on flat quartz or

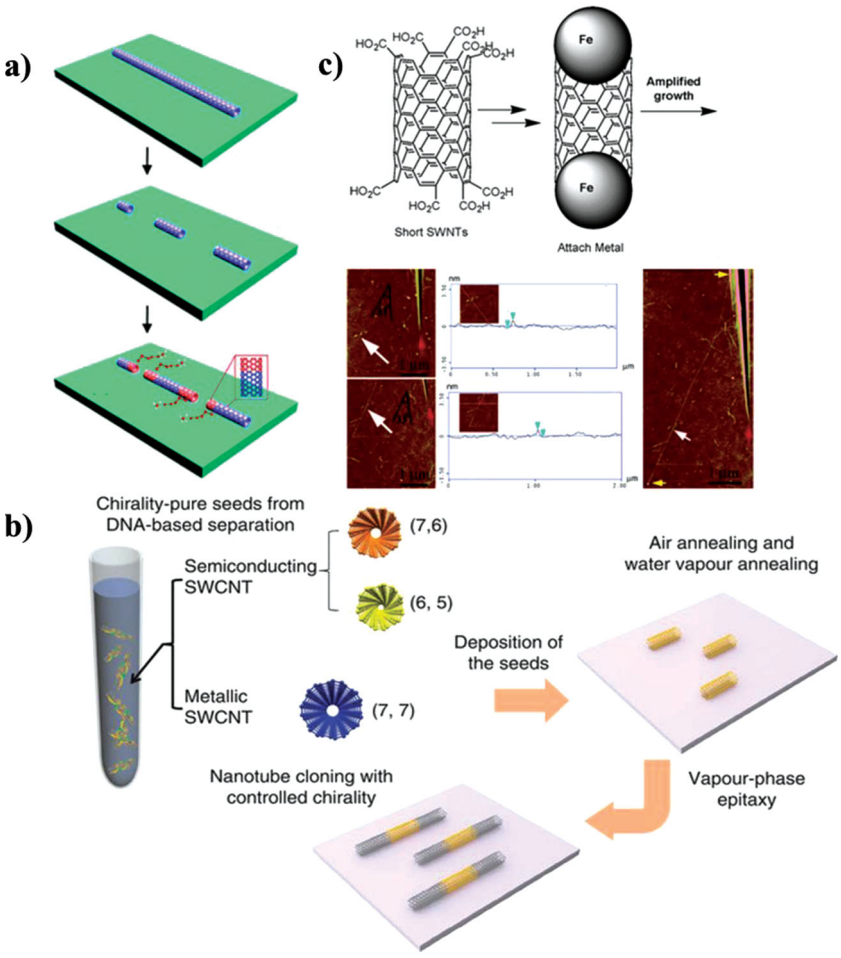

Figure 17. a) Schematic diagrams of cloning process for as-grown ultra-long SWNTs. Reproduced with permission.[92] Copyright 2009, American Chemical Society. b) Schematic illustration of the vapor-phase epitaxy (VPE) process for chirality controlled SWNT synthesis. Reproduced with permission.[175] Copyright 2002, Nature Publishing Group. c) Schematic diagrams of substantial growth through reloaded Fe nanoparticles. Reproduced with permission.[173] Copyright 2006, American Chemical Society.

sapphire surface is normally smaller than the real value due to the SWNT-substrate interaction. SEM is usually used to characterize the macro morphology and length of SWNTs, and the obtaining of high quality images extremely rely on the use of conducting substrates. Unfortunately, all of these techniques cannot be used to characterize the chiral structure.

9.1. Strategies to Identify the Chirality

The inherent linkage between chiral index and intrinsic structures of SWNT is crucial to develop an efficient and reliable characterization approach.[178,179] As we know, the rolling vector (n,m) of SWNT completely determines the diameter (d), chiral angle (θ), handedness, and electron transition energy (E_{ii}, i is an integer): $d = a\,(n^2 + nm + m^2)^{1/2}\pi$ (a is the C–C length), $\theta = \tan^{-1}[((3)^{1/2}m)/(2n + m)]$ and $E_{ii} = f(n,m)$. Moreover, for a given SWNT, its van Hove transitions between energy bands endue the E_{ii} with different values. SWNT enantiomers of $n > m$ and $m > n$ are right (R-) and left (L-) handed, respectively, which share the identical d and $\theta_R + \theta_L = 60°$. In this way, the (n,m) index can be mathematically deduced if any two parameters of d, θ, E_{ii}, and $E_{i'i'}$ (i and i' are different integers) are obtained. Furthermore, the characterization methods can be classified into four categories: (θ, d), (d, E_{ii}), (θ, E_{ii}), and (E_{ii}, $E_{i'i'}$), which absolutely sweeps all present methods, as shown in **Figure 18**a. Furthermore, four related plots can be drawn to conveniently assign the n and m values, including (θ, d), (d, E_{ii}), (θ, E_{ii}), and (E_{ii}, $E_{i'i'}$) plots. Of which, (d, E_{ii}) plot is well known as

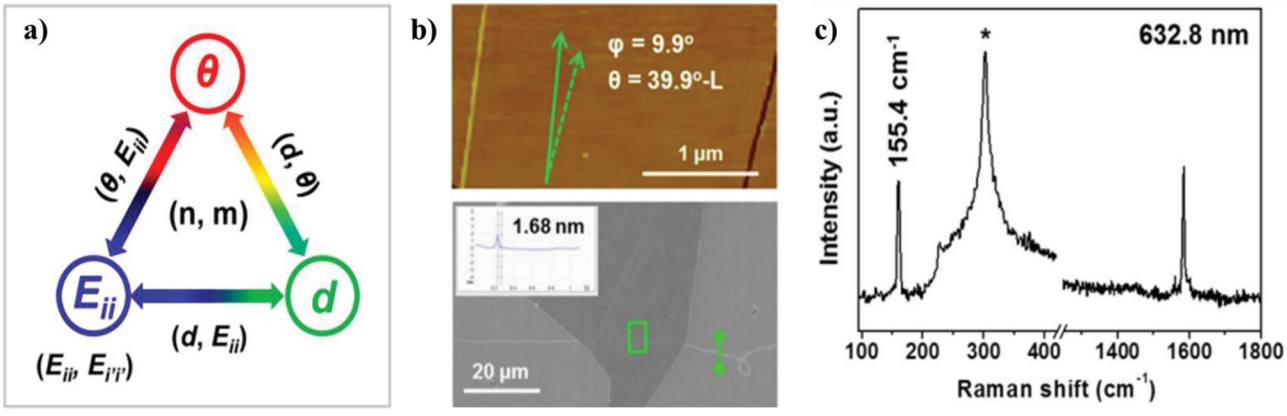

Figure 18. a) Strategy for the chiral structure determinations of SWNTs, which contains four types of (θ, d), (d, E_{ii}), (θ, E_{ii}), and (E_{ii}, $E_{i'i'}$). b) The typical AFM image (up panel) and SEM image (below panel) of obtained SWNTs on graphite surfaces. c) Raman spectra of SWNT in (b), and the laser wavelength is 632.8 nm. (a-c) are reproduced with permission.[177] Copyright 2013, American Chemical Society.

Kataura-plot,[180] and it has already been used in resonance Raman spectroscopy (RRS).[181] (*n*,*m*) assignments of SWNTs by photoluminescence excitation (PLE) spectroscopy[182] and Rayleigh Scattering spectroscopy (RSS)[183] depend on the (E_{ii}, $E_{i'i'}$) plot. There were rare exploration on (θ, d) and (θ, E_{ii}) plots.

Corresponding to the above strategy, four related plots can be drawn to conveniently assign the *n* and *m* values, including (θ, d), (d, E_{ii}), (θ, E_{ii}), and (E_{ii}, $E_{i'i'}$) plots. Of which, (d, E_{ii}) plot is well known as Kataura-plot,[180] and it has already been used in RRS.[181] (*n*,*m*) assignments of SWNTs by PLE spectroscopy[182] and RSS[183] depend on the (E_{ii}, $E_{i'i'}$) plot. J. Zhang's group put forward both the (θ, d) and (θ, E_{ii}) plots as shown in **Figure 19**a and 19b, respectively.[177] Distinctly, these two plots supplied plenty of structural information, such as R-handed, L-handed, s- and m- SWNTs. It is mentioned that SWNTs on the violet, blue, green, and black/red lines exhibit the same *n*, *m*, (*n* + *m*), and (n − *m*) values, respectively. Furthermore, (θ, d) plots remedy the drawback of Kataura-plot, which is unavailable to SWNT with large diameter.

9.2. Conventional Approaches

STM, HRTEM, selected-area electron diffraction (ED),[184] RRS, RSS and PLE, as the conventional methods, have already been extensively used to characterize the chiral structures of SWNTs, all of which are involved into the relational graph (Figure 18a). Obviously, the methods in (θ, d) type simultaneously require the θ and d information, which requires technique such as STM, HRTEM and ED. Although the atomic structures of an individual SWNT can be obtained by these microscopic techniques, each of which requires rigorous conditions and prohibitive costs. For example, groups of Lieber C.M. and Dekker C. acquired the perfect STM images with atomic resolution,[5,185] and further verified the theoretical predication that energy gap of SWNT inversely varied with its diameter. The status of STM probe, conductivity and cleanness of samples were critical to generate the stable tunneling current. These methods are unable to characterize SWNTs on a large scale.

In contrast, spectroscopic techniques such as RRS, RSS and PLE are able to characterize specimens in a large scale. RRS belongs to (d, E_{ii}) type and can provide numerous property and structure information of SWNTs, including d, electronical type and E_{ii} values.[186] Low frequency of radial breathing mode (RBM) of SWNT is inversely proportional to its diameter with $\omega_{RBM} = C/d$ (cm^{-1}) (C = 248 cm^{-1} nm for SiO_x substrate). ω_{RBM} shifts sensitively depend on the laser energies, which can be used to distinguish s- or m- SWNTs. However, continuous laser excitations are necessary to match the resonance window of each SWNTs. Moreover, (n,m) index can be extracted from Kataura-plot by using (d, E_{ii}) plot. The appearance of D band at 1350 cm^{-1} indicates the SWNTs are defective or damaged. G band around 1580 cm^{-1} is normally split into two features, G^+ at 1590 cm^{-1} and G^- at 1570 cm^{-1}. The Breit–Wigner–Fano and Lorentzian lineshapes of G^- mode can indicate m- or and s-SWNTs, respectively. Besides, RSS and PLE as the typical methods belong to (E_{ii}, $E_{i'i'}$) type. In brief, RSS is limited by the suspended SWNTs. PLE is only suitable for the s-SWNTs with small diameters. As we know, the band structures of SWNT sensitively depend on its surrounding environments, such as temperature, substrate and possible contaminations. As such, methods in (E_{ii}, $E_{i'i'}$) and (d, E_{ii}) types cannot well serve the bundled and surfactant wrapped samples. Also, the above conventional methods can not determine the handedness and chiral angle of SWNTs. A convenient and accurate approach to comprehensively characterize the chiral structures of SWNTs is highly desirable.

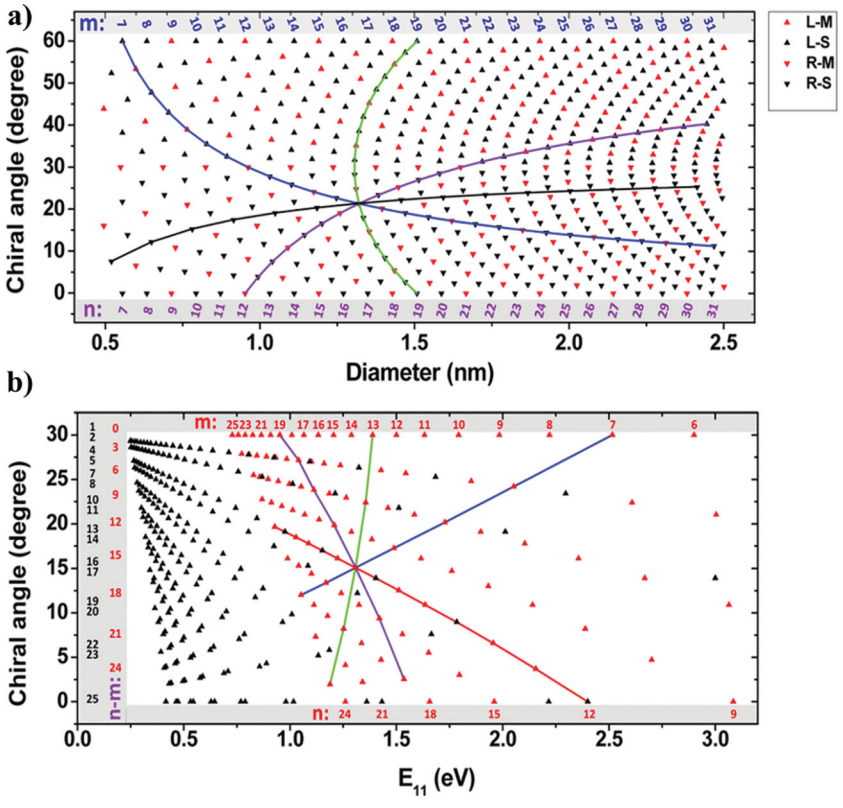

Figure 19. a) The (θ, d) plot. b) The (θ, E_{ii}) plot for chiral structure assignment. The upward-pointing, downward-pointing, red, and black triangles refer to the L-, R-, m-, and s- SWNTs, respectively. Moreover, the SWNTs on violet, blue, green, and black/red lines share the identical n, m, (n + m), and (n − m) values, respectively. The intersections of four lines in (a) and (b) are (12,7)-R-S and (19,7)-R-M SWNTs, respectively. (a) and (b) are reproduced with permission.[177] Copyright 2013, American Chemical Society.

9.3. Chirality Identification of SWNTs using Graphite as a Reference

As described in Section 3, the orientation of as-grown SWNTs on graphite surface shows chirality-selectivity. In this way, AC, ZZ and chiral SWNTs are aligned along the

ZZ, AC and chiral edges of graphene, respectively. The R- and L- SWNTs are distributed in different graphene segments. Therefore, the benzene ring arrangements of graphene could indicate the chiral structures of aligned SWNTs on it. After the CVD process, many graphene trenches appeared due to the etching effect of metallic nanoparticles. Importantly, these trenches are mostly along ZZ directions according to STM and Raman measurements.[187] Using these trenches as reference, we developed a novel approach to determine the handedness, chiral angle and even (*n*,*m*) index of the aligned SWNTs on graphite surfaces.

Handedness and especially chiral angle are the key factors for methods based on (θ, d) and (θ, E_{ii}). Specifically, if the graphene trenches arise in the counter-clockwise (clockwise) direction of SWNT and their formed angle φ ranges $0° < \varphi_R < 30°$ ($30° < \varphi_{R'} < 60°$), then the SWNTs are right-handed with chiral angle of $\theta_R = 30° - \varphi_R$ ($\theta_R = \varphi_R - 30°$). In contrast, if the graphene trenches are shown in the clockwise (counter-clockwise) direction of SWNT and the angle φ ranges $0° < \varphi_L < 30°$ ($30° < \varphi_{L'} < 60°$), then the SWNTs are left-handed with chiral angle of $\theta_L = 30° + \varphi_L$ ($\theta_L = 90° - \varphi_L$).[174] Taking the SWNT in Figure 18b as an example, SWNT was aligned in the counter-clockwise direction of graphene trench, and the formed angle φ is 9.9°. So, this SWNT is left-handed with $\theta_L = 39.9°$. Both AFM profile and RBM band (Figure 18b and 18c) were used to evaluate its diameter, approximating 1.68 nm. Finally, the (n,m) index can be easily assigned to (8,15)-L-S through the (θ, d) plot. Meanwhile, E_{ii} value can be measured by the anti-Stokes/Stokes resonant Raman intensity ratio, which validate the (θ, E_{ii}) plot to determine chiral structures. Obviously, this novel approach presents many applicable merits of high-efficiency, large-scale and low-cost.

10. Conclusions and Outlook

Due to the fact that the properties of SWNTs tightly dependent on their structures, the synthesis of SWNTs with controlled structures, especially direct on surfaces, are of high importance for the fabrication of SWNT-based nanoelectronics. In the recent ten years, great successes have been achieved in the field. CVD is the most promising and controllable approach to synthesis SWNTs on surfaces. The structures of the SWNTs produced by CVD are influenced by many factors, among which the catalyst nanoparticles play the most important role. To date, various catalysts, including metallic and non-metallic ones, have been proved to be catalytic active in the growth of SWNTs, and several different catalytic mechanisms, including VLS, VS and VSSS, have been proposed. And depending on the interaction between the catalyst and substrate surface, the growth mode could be tip- or base- growth, as evidenced by in situ TEM.

The direction of the SWNTs during its growth could be controlled by gas flow, the SWNT-surface interactions, or external fields, which could be used to prepare horizontally aligned SWNT arrays, and further to construct complex assembly structures, such as cross-bars and serpentine of SWNTs. Using optimized CVD conditions, the aligned SWNTs on the surface have been observed to grow at a very high rate, up to 5 mm/min, facilitate the prepare of ultra-long SWNTs. Up to date, 55 cm-long few-walled CNTs, including SWNTs, have been achieved. Besides, nano-barriers can be introduced into the CVD process to stop the extension of SWNTs to get SWNTs to a certain length. For the number density of aligned SWNTs on surfaces, IBM proposed an optimal requirement as 125 SWNTs/μm, which encouraging people to improve the process. The density SWNTs are governed by the density of active catalysts, and have been improved by using optimal catalyst treatment, multi-cycle CVD, or post multiple transfer process. A density of 55 SWNTs/μm has been achieved.

The diameters of SWNTs highly depend on catalysts. By choosing catalysts with a certain size, SWNTs with diameters in a small range could be selectively grown. For a certain catalyst nanoparticle, temperature also influences the diameters of SWNTs, according to what, the modulation of diameters of a SWNT during its growth has been exhibited. Besides, the gas feedings are also proved to affect the diameters of SWNTs. Various in situ or post growth methods have been developed to get pure semiconducting or metallic SWNTs. SWNTs with more than 97% of semiconducting or more than 90% metallic SWNTs have been successfully prepared. The chirality control is the most challenging issue. Considering the different growth rate of SWNTs with different chirality, the selectively growth of SWNTs with certain chiralities could be obtained. And by using of catalyst nanoparticles with specific structures, SWNTs with some certain chirality could be produced. Besides, cap engineering or cloning are also promising for the chirality controlled growth. Further, to determining the chirality of SWNTs, a method based graphite or graphene has been developed beyond the conventional method such TEM, RRS and PLE.

In spite of these achievements, great challenges still remain. Chirality controlled growth of SWNTs is still the biggest challenge, although some approaches have been developed to control the chirality of as-synthesized SWNTs, such as cloning or cap engineering, which efficiency are quite low. Designing the catalysts is the most straight forward method to realize the large scale synthesis of chirality-controlled SWNTs. It is important to in situ investigate the crystalline structures of the catalyst nanoparticles and the catalyst-SWNT interfaces during the growth of SWNTs, which could guide the design of catalysts. Another promising approach is to scale up the "cloning" of SWNTs with pre-separated SWNTs with the same chirality as the seeds. Ultra-long SWNTs, with their uniform structures along the axis, could also be used to create multiple SWNT segments with the same chirality and diameter. Besides, the density of aligned SWNTs on surfaces is still not high enough for the requirements of integrated electronics. Breakthroughs in the directly CVD growth of dense SWNTs or post-growth non-destructive transfer technique are in demand.

Acknowledgements

This work was supported by MOST (2011CB932601, 2013CB934200, 2011YQ0301240201) and NSFC (21233001, 51121091, 21129001, 21203107, 51372132, 51272006).

Received: January 27, 2014
Revised: May 25, 2014
Published online: July 17, 2014

[1] M. F. L. De Volder, S. H. Tawfick, R. H. Baughman, A. J. Hart, *Science* **2013**, *339*, 535.
[2] P. L. McEuen, M. S. Fuhrer, H. K. Park, *IEEE T. Nanotechnol.* **2002**, *1*, 78.
[3] M. Terrones, *Annu. Rev. Mater. Res.* **2003**, *33*, 419.
[4] Q. Zhang, J. Q. Huang, W. Z. Qian, Y. Y. Zhang, F. Wei, *Small* **2013**, *9*, 1237.
[5] S. J. Tans, A. R. M. Verschueren, C. Dekker, *Nature* **1998**, *393*, 49.
[6] Z. Y. Zhang, S. Wang, L. Ding, X. L. Liang, T. Pei, J. Shen, H. L. Xu, O. Chen, R. L. Cui, Y. Li, L. M. Peng, *Nano Lett.* **2008**, *8*, 3696.
[7] Z. H. Chen, J. Appenzeller, Y. M. Lin, J. Sippel-Oakley, A. G. Rinzler, J. Y. Tang, S. J. Wind, P. M. Solomon, P. Avouris, *Science* **2006**, *311*, 1735.
[8] M. M. Shulaker, G. Hills, N. Patil, H. Wei, H. Y. Chen, H. S. PhilipWong, S. Mitra, *Nature* **2013**, *501*, 526.
[9] D. S. Bethune, C. H. Kiang, M. S. Devries, G. Gorman, R. Savoy, J. Vazquez, R. Beyers, *Nature* **1993**, *363*, 605.
[10] S. Iijima, T. Ichihashi, *Nature* **1993**, *363*, 603.
[11] T. W. Ebbesen, P. M. Ajayan, *Nature* **1992**, *358*, 220.
[12] S. Lebedkin, F. Hennrich, T. Skipa, M. M. Kappes, *J. Phys. Chem. B* **2003**, *107*, 1949.
[13] M. Endo, K. Takeuchi, S. Igarashi, K. Kobori, M. Shiraishi, H. W. Kroto, *J. Phys. Chem. Solids* **1993**, *54*, 1841.
[14] Y. Li, R. Cui, L. Ding, Y. Liu, W. Zhou, Y. Zhang, Z. Jin, F. Peng, J. Liu, *Adv. Mater.* **2010**, *22*, 1508.
[15] J. Kong, A. M. Cassell, H. Dai, *Chem. Phys. Lett.* **1998**, *292*, 567.
[16] M. Mayne, N. Grobert, M. Terrones, R. Kamalakaran, M. Rühle, H. W. Kroto, D. R. M. Walton, *Chem. Phys. Lett.* **2001**, *338*, 101.
[17] J. C. Hamilton, J. M. Blakely, *Surf. Sci.* **1980**, *91*, 199.
[18] D. Takagi, Y. Homma, H. Hibino, S. Suzuki, Y. Kobayashi, *Nano Lett.* **2006**, *6*, 2642.
[19] D. Yuan, L. Ding, H. Chu, Y. Feng, T. P. McNicholas, J. Liu, *Nano Lett.* **2008**, *8*, 2576.
[20] W. Yang, K. R. Ratinac, S. P. Ringer, P. Thordarson, J. J. Gooding, F. Braet, *Angew. Chem. Int. Edit.* **2010**, *49*, 2114.
[21] V. Derycke, R. Martel, M. Radosavljevi, F. M. Ross, P. Avouris, *Nano Lett.* **2002**, *2*, 1043.
[22] D. Takagi, H. Hibino, S. Suzuki, Y. Kobayashić, Y. Homma, *Nano Lett.* **2007**, *7*, 2272.
[23] A. I. Persson, M. W. Larsson, S. Stenstrom, B. J. Ohlsson, L. Samuelson, L. R. Wallenberg, *Nat. Mater.* **2004**, *3*, 677.
[24] D. Takagi, Y. Kobayashi, Y. Homma, *J. Am. Chem. Soc.* **2009**, *131*, 6922.
[25] S. Huang, Q. Cai, J. Chen, Y. Qian, L. Zhang, *J. Am. Chem. Soc.* **2009**, *131*, 2094.
[26] B. Liu, W. Ren, C. Liu, C.-H. Sun, L. Gao, S. Li, C. Jiang, H.-M. Cheng, *ACS Nano* **2009**, *3*, 3421.
[27] B. Liu, D.-M. Tang, C. Sun, C. Liu, W. Ren, F. Li, W.-J. Yu, L.-C. Yin, L. Zhang, C. Jiang, H.-M. Cheng, *J. Am. Chem. Soc.* **2010**, *133*, 197.
[28] R. S. Wagner, W. C. Ellis, *Appl. Phys. Lett.* **1964**, *4*, 89.
[29] J. Kong, H. T. Soh, A. M. Cassell, C. F. Quate, H. Dai, *Nature* **1998**, *395*, 878.
[30] S. Hofmann, G. Csányi, A. C. Ferrari, M. C. Payne, J. Robertson, *Phys. Rev. Lett.* **2005**, *95*, 036101.
[31] B. Liu, W. Ren, L. Gao, S. Li, S. Pei, C. Liu, C. Jiang, H.-M. Cheng, *J. Am. Chem. Soc.* **2009**, *131*, 2082.
[32] Y. Chen, J. Zhang, *Carbon* **2011**, *49*, 3316.
[33] S. Helveg, C. Lopez-Cartes, J. Sehested, P. L. Hansen, B. S. Clausen, J. R. Rostrup-Nielsen, F. Abild-Pedersen, J. K. Norskov, *Nature* **2004**, *427*, 426.
[34] H. Yoshida, S. Takeda, T. Uchiyama, H. Kohno, Y. Homma, *Nano Lett.* **2008**, *8*, 2082.
[35] S. J. Kang, C. Kocabas, T. Ozel, M. Shim, N. Pimparkar, M. A. Alam, S. V. Rotkin, J. A. Rogers, *Nat. Nanotechnol.* **2007**, *2*, 230.
[36] H. Park, A. Afzali, S. J. Han, G. S. Tulevski, A. D. Franklin, J. Tersoff, J. B. Hannon, W. Haensch, *Nat. Nanotechnol.* **2012**, *7*, 787.
[37] C. Kocabas, S. H. Hur, A. Gaur, M. A. Meitl, M. Shim, J. A. Rogers, *Small* **2005**, *1*, 1110.
[38] A. D. Franklin, *Nature* **2013**, *498*, 443.
[39] X. L. Li, L. Zhang, X. R. Wang, I. Shimoyama, X. M. Sun, W. S. Seo, H. J. Dai, *J. Am. Chem. Soc.* **2007**, *129*, 4890.
[40] G. H. Yu, A. Y. Cao, C. M. Lieber, *Nat. Nanotechnol.* **2007**, *2*, 372.
[41] Y. N. Zhang, L. X. Zheng, *Nanoscale* **2010**, *2*, 1919.
[42] I. Ibrahim, A. Bachmatiuk, J. H. Warner, B. Buchner, G. Cuniberti, M. H. Rummeli, *Small* **2012**, *8*, 1973.
[43] W. Z. Li, S. S. Xie, L. X. Qian, B. H. Chang, B. S. Zou, W. Y. Zhou, R. A. Zhao, G. Wang, *Science* **1996**, *274*, 1701.
[44] S. M. Huang, B. Maynor, X. Y. Cai, J. Liu, *Adv. Mater.* **2003**, *15*, 1651.
[45] M. Su, Y. Li, B. Maynor, A. Buldum, J. P. Lu, J. Liu, *J. Phys. Chem. B.* **2000**, *104*, 6505.
[46] A. Ismach, L. Segev, E. Wachtel, E. Joselevich, *Angew. Chem. Int. Edit.* **2004**, *43*, 6140.
[47] Y. G. Zhang, A. L. Chang, J. Cao, Q. Wang, W. Kim, Y. M. Li, N. Morris, E. Yenilmez, J. Kong, H. J. Dai, *Appl. Phys. Lett.* **2001**, *79*, 3155.
[48] V. Jourdain, C. Bichara, *Carbon* **2013**, *58*, 2.
[49] S. Han, X. L. Liu, C. W. Zhou, *J. Am. Chem. Soc.* **2005**, *127*, 5294.
[50] A. Ismach, D. Kantorovich, E. Joselevich, *J. Am. Chem. Soc.* **2005**, *127*, 11554.
[51] S. M. Huang, M. Woodson, R. Smalley, J. Liu, *Nano Lett.* **2004**, *4*, 1025.
[52] B. H. Peng, S. Jiang, Y. Y. Zhang, J. Zhang, *Carbon* **2011**, *49*, 2555.
[53] G. Hong, Y. B. Chen, P. Li, J. Zhang, *Carbon* **2012**, *50*, 2067.
[54] E. Joselevich, *Nano Res.* **2009**, *2*, 743.
[55] A. Ismach, E. Joselevich, *Nano Lett.* **2006**, *6*, 1706.
[56] N. Geblinger, A. Ismach, E. Joselevich, *Nat. Nanotechnol.* **2008**, *3*, 195.
[57] Q. Wen, R. F. Zhang, W. Z. Qian, Y. R. Wang, P. H. Tan, J. Q. Nie, F. Wei, *Chem. Mater.* **2010**, *22*, 1294.
[58] M. Hofmann, D. Nezich, A. Reina, J. Kong, *Nano Lett.* **2008**, *8*, 4122.
[59] Z. Jin, H. B. Chu, J. Y. Wang, J. X. Hong, W. C. Tan, Y. Li, *Nano Lett.* **2007**, *7*, 2073.
[60] L. X. Zheng, M. J. O'Connell, S. K. Doorn, X. Z. Liao, Y. H. Zhao, E. A. Akhadov, M. A. Hoffbauer, B. J. Roop, Q. X. Jia, R. C. Dye, D. E. Peterson, S. M. Huang, J. Liu, Y. T. Zhu, *Nat. Mater.* **2004**, *3*, 673.
[61] R. F. Zhang, Y. Y. Zhang, Q. Zhang, H. H. Xie, W. Z. Qian, F. Wei, *ACS Nano* **2013**, *7*, 6156.
[62] R. F. Zhang, H. H. Xie, Y. Y. Zhang, Q. Zhang, Y. G. Jin, P. Li, W. Z. Qian, F. Wei, *Carbon* **2013**, *52*, 232.
[63] Y. Homma, H. P. Liu, D. Takagi, Y. Kobayashi, *Nano Res.* **2009**, *2*, 793.
[64] H. H. Xie, R. F. Zhang, Y. Y. Zhang, P. Li, Y. G. Jin, F. Wei, *Carbon* **2013**, *52*, 535.
[65] W. W. Zhou, Z. Y. Han, J. Y. Wang, Y. Zhang, Z. Jin, X. Sun, Y. W. Zhang, C. H. Yan, Y. Li, *Nano Lett.* **2006**, *6*, 2987.
[66] B. Zhang, G. Hong, B. Peng, J. Zhang, W. Choi, J. M. Kim, J. Y. Choi, Z. Liu, *J. Phys. Chem. C* **2009**, *113*, 5341.
[67] H. Ago, K. Nakamura, K. Ikeda, N. Uehara, N. Ishigami, M. Tsuji, *Chem. Phys. Lett.* **2005**, *408*, 433.
[68] C. M. Orofeo, H. Ago, T. Ikuta, K. Takahasi, M. Tsuji, *Nanoscale* **2010**, *2*, 1708.
[69] D. Tsivion, M. Schvartzman, R. Popovitz-Biro, P. von Huth, E. Joselevich, *Science* **2011**, *333*, 1003.
[70] D. Tsivion, M. Schvartzman, R. Popovitz-Biro, E. Joselevich, *ACS Nano* **2012**, *6*, 6433.

[71] L. Ding, D. N. Yuan, J. Liu, *J. Am. Chem. Soc.* **2008**, *130*, 5428.
[72] H. Ago, K. Imamoto, N. Ishigami, R. Ohdo, K. Ikeda, M. Tsuji, *Appl. Phys. Lett.* **2007**, *90*, 123112.
[73] S. Jeong, A. Oshiyama, *Phys. Rev. Lett.* **2011**, *107*, 065501.
[74] X. L. Liu, K. Ryu, A. Badmaev, S. Han, C. W. Zhou, *J. Phys. Chem. C* **2008**, *112*, 15929.
[75] B. Wang, Y. F. Ma, N. Li, Y. P. Wu, F. F. Li, Y. S. Chen, *Adv. Mater.* **2010**, *22*, 3067.
[76] L. Y. Jiao, B. Fan, X. J. Xian, Z. Y. Wu, J. Zhang, Z. F. Liu, *J. Am. Chem. Soc.* **2008**, *130*, 12612.
[77] N. Patil, A. Lin, E. R. Myers, K. Ryu, K. A. Badmaev, C. W. Zhou, H. S. P. Wong, S. Mitra, *IEEE Trans. Nanotechnol.* **2009**, *8*, 498.
[78] Y. G. Yao, X. C. Dai, C. Q. Feng, J. Zhang, X. L. Liang, L. Ding, W. Choi, J. Y. Choi, J. M. Kim, Z. F. Liu, *Adv. Mater.* **2009**, *21*, 4158.
[79] Y. B. Chen, Y. Hu, Y. Fang, P. Li, C. Q. Feng, J. Zhang, *Carbon* **2012**, *50*, 3295.
[80] Y. Chen, Z. Shen, Z. Xu, Y. Hu, H. Xu, S. Wang, X. Guo, Y. Zhang, L. Peng, F. Ding, Z. Liu, J. Zhang, *Nat. Commun.* **2013**, *4*, 2205.
[81] K. S. Novoselov, A. K. Geim, S. V. Morozov, D. Jiang, Y. Zhang, S. V. Dubonos, I. V. Grigorieva, A. A. Firsov, *Science* **2004**, *306*, 666.
[82] J. Li, Y. He, Y. Han, K. Liu, J. Wang, Q. Li, S. Fan, K. Jiang, *Nano Lett.* **2012**, *12*, 4095.
[83] R. Zhang, Y. Zhang, Q. Zhang, H. Xie, H. Wang, J. Nie, Q. Wen, F. Wei, *Nat. Commun.* **2013**, *4*, 1727.
[84] N. Mingo, D. Broido, *Nano Lett.* **2005**, *5*, 1221.
[85] Z. L. Wang, D. W. Tang, X. B. Li, X. H. Zheng, W. G. Zhang, L. X. Zheng, Y. T. Zhu, A. Z. Jin, H. F. Yang, C. Z. Gu, *Appl. Phys. Lett.* **2007**, *91*, 123119.
[86] A. D. Franklin, Z. Chen, *Nat. Nanotechnol.* **2010**, *5*, 858.
[87] B. C. Edwards, *Acta Astronautica* **2000**, *47*, 735.
[88] J. Martinez, T. D. Yuzvinsky, A. M. Fennimore, A. Zettl, R. García, C. Bustamante, *Nanotechnology* **2005**, *16*, 2493.
[89] J. H. Hafner, C.-L. Cheung, T. H. Oosterkamp, C. M. Lieber, *J. Phys. Chem. B* **2001**, *105*, 743.
[90] S. R. Lustig, E. D. Boyes, R. H. French, T. D. Gierke, M. A. Harmer, P. B. Hietpas, A. Jagota, R. S. McLean, G. P. Mitchell, G. B. Onoa, *Nano Lett.* **2003**, *3*, 1007.
[91] I. Stepanek, G. Maurin, P. Bernier, J. Gavillet, A. Loiseau, R. Edwards, O. Jaschinski, *Chem.Phys. Lett.* **2000**, *331*, 125.
[92] Y. Yao, C. Feng, J. Zhang, Z. Liu, *Nano Lett.* **2009**, *9*, 1673.
[93] K. J. Ziegler, Z. Gu, J. Shaver, Z. Chen, E. L. Flor, D. J. Schmidt, C. Chan, R. H. Hauge, R. E. Smalley, *Nanotechnology* **2005**, *16*, S539.
[94] Z. Gu, H. Peng, R. Hauge, R. Smalley, J. Margrave, *Nano Lett.* **2002**, *2*, 1009.
[95] C. Feng, Y. Yao, J. Zhang, Z. Liu, *Nano Res.* **2009**, *2*, 768.
[96] R. Zhang, Y. Zhang, Q. Zhang, H. Xie, W. Qian, F. Wei, *ACS Nano* **2013**, *7*, 6156.
[97] B. H. Hong, J. Y. Lee, T. Beetz, Y. Zhu, P. Kim, K. S. Kim, *J. Am. Chem. Soc.* **2005**, *127*, 15336.
[98] X. Wang, Q. Li, J. Xie, Z. Jin, J. Wang, Y. Li, K. Jiang, S. Fan, *Nano Lett.* **2009**, *9*, 3137.
[99] W. Kim, H. C. Choi, M. Shim, Y. Li, D. Wang, H. Dai, *Nano Lett.* **2002**, *2*, 703.
[100] C. Kocabas, S. J. Kang, T. Ozel, M. Shim, J. A. Rogers, *J. Phys. Chem. C* **2007**, *111*, 17879.
[101] K. Hata, D. N. Futaba, K. Mizuno, T. Namai, M. Yumura, S. Iijima, *Science* **2004**, *306*, 1362.
[102] A. J. Hart, A. H. Slocum, L. Royer, *Carbon* **2006**, *44*, 348.
[103] J. Park, J. Yoon, S. J. Kang, G. T. Kim, J. S. Ha, *Carbon* **2011**, *49*, 2492.
[104] I. J. Teng, K. L. Chen, H. L. Hsu, S. R. Jian, L. C. Wang, J. H. Chen, W. H. Wang, C. T. Kuo, *J. Phys. D: Appl. Phys.* **2011**, *44*, 145401.
[105] J. P. Edgeworth, N. R. Wilson, J. V. Macpherson, *Small* **2007**, *3*, 860.
[106] Z. Liu, L. Jiao, Y. Yao, X. Xian, J. Zhang, *Adv. Mater.* **2010**, *22*, 2285.
[107] J. L. Xiao, S. Dunham, P. Liu, Y. W. Zhang, C. Kocabas, L. Moh, Y. G. Huang, K. C. Hwang, C. Lu, W. Huang, J. A. Rogers, *Nano Lett.* **2009**, *9*, 4311.
[108] J. H. Li, K. H. Liu, S. B. Liang, W. W. Zhou, M. Pierce, F. Wang, L. M. Peng, J. Liu, *Acs Nano* **2014**, *8*, 554.
[109] D. N. Futaba, K. Hata, T. Namai, T. Yamada, K. Mizuno, Y. Hayamizu, M. Yumura, S. Iijima, *J. Phys. Chem. B* **2006**, *110*, 8035.
[110] W. W. Zhou, L. Ding, S. Yang, J. Liu, *ACS Nano* **2011**, *5*, 3849.
[111] S. W. Hong, T. Banks, J. A. Rogers, *Adv. Mater.* **2010**, *22*, 1826.
[112] H. Ago, N. Uehara, K.-i. Ikeda, R. Ohdo, K. Nakamura, M. Tsuji, *Chem. Phys. Lett.* **2006**, *421*, 399.
[113] H. Ago, Y. Nakamura, Y. Ogawa, M. Tsuji, *Carbon* **2011**, *49*, 176.
[114] C. A. Wang, K. M. Ryu, L. G. De Arco, A. Badmaev, J. L. Zhang, X. Lin, Y. C. Che, C. W. Zhou, *Nano Res.* **2010**, *3*, 831.
[115] H. Dai, A. G. Rinzler, P. Nikolaev, A. Thess, D. T. Colbert, R. E. Smalley, *Chem. Phys. Lett.* **1996**, *260*, 471.
[116] S. B. Sinnott, R. Andrews, D. Qian, A. M. Rao, Z. Mao, E. C. Dickey, F. Derbyshire, *Chem. Phys. Lett.* **1999**, *315*, 25.
[117] P. E. Anderson, N. M. Rodríguez, *Chem. Mater.* **2000**, *12*, 823.
[118] C. L. Cheung, J. H. Hafner, C. M. Lieber, *Proc. Natl. Aacd. Sci. USA* **2000**, *97*, 3809.
[119] Y. Li, W. Kim, Y. Zhang, M. Rolandi, D. Wang, H. Dai, *J. Phys. Chem. B* **2001**, *105*, 11424.
[120] A. M. Cassell, J. A. Raymakers, J. Kong, H. Dai, *J. Phys. Chem. B* **1999**, *103*, 6484.
[121] H. Omachi, T. Nakayama, E. Takahashi, Y. Segawa, K. Itami, *Nature Chem.* **2013**, *5*, 572.
[122] C. L. Cheung, A. Kurtz, H. Park, C. M. Lieber, *J. Phys. Chem. B* **2002**, *106*, 2429.
[123] L. An, J. M. Owens, L. E. McNeil, J. Liu, *J. Am. Chem. Soc.* **2002**, *124*, 13688.
[124] A. Müller, S. K. Das, P. Kögerler, H. Bögge, M. Schmidtmann, A. X. Trautwein, V. Schünemann, E. Krickemeyer, W. Preetz, *Angew. Chem. Int. Ed.* **2000**, *39*, 3413.
[125] A. Muller, S. K. Das, H. Bogge, M. Schmidtmann, A. Botar, A. Patrut, *Chem. Comm.* **2001**, 657.
[126] C. Lu, J. Liu, *J. Phys. Chem. B* **2006**, *110*, 20254.
[127] Y. Yao, X. Dai, R. Liu, J. Zhang, Z. Liu, *J. Phys. Chem. C* **2009**, *113*, 13051.
[128] G. Zhang, D. Mann, L. Zhang, A. Javey, Y. Li, E. Yenilmez, Q. Wang, J. P. McVittie, Y. Nishi, J. Gibbons, H. Dai, *P. Natl. Aacd. Sci. USA* **2005**, *102*, 16141.
[129] Z. Zhu, H. Jiang, T. Susi, A. G. Nasibulin, E. I. Kauppinen, *J. Am. Chem. Soc.* **2010**, *133*, 1224.
[130] L. Ding, A. Tselev, J. Wang, D. Yuan, H. Chu, T. P. McNicholas, Y. Li, J. Liu, *Nano Lett.* **2009**, *9*, 800.
[131] J. Lu, S. Nagase, X. W. Zhang, D. Wang, M. Ni, Y. Maeda, T. Wakahara, T. Nakahodo, T. Tsuchiya, T. Akasaka, Z. X. Gao, D. P. Yu, H. Q. Ye, W. N. Mei, Y. S. Zhou, *J. Am. Chem. Soc.* **2006**, *128*, 5114.
[132] W. W. Zhou, S. T. Zhan, L. Ding, J. Liu, *J. Am. Chem. Soc.* **2012**, *134*, 14019.
[133] X. F. Feng, S. W. Chee, R. Sharma, K. Liu, X. Xie, Q. Q. Li, S. S. Fan, K. L. Jiang, *Nano Res.* **2011**, *4*, 767.
[134] Y. M. Li, D. Mann, M. Rolandi, W. Kim, A. Ural, S. Hung, A. Javey, J. Cao, D. W. Wang, E. Yenilmez, Q. Wang, J. F. Gibbons, Y. Nishi, H. J. Dai, *Nano Lett.* **2004**, *4*, 317.
[135] G. Hong, B. Zhang, B. H. Peng, J. Zhang, W. M. Choi, J. Y. Choi, J. M. Kim, Z. F. Liu, *J. Am. Chem. Soc.* **2009**, *131*, 14642.
[136] W.-J. Kim, M. L. Usrey, M. S. Strano, *Chem. Mater.* **2007**, *19*, 1571.
[137] X. Tu, M. Zheng, *Nano Res.* **2008**, *1*, 185.
[138] Y. Zhang, Y. Zhang, X. Xian, J. Zhang, Z. Liu, *J. Phys. Chem. C* **2008**, *112*, 3849.

[139] K. Moshammer, F. Hennrich, M. Kappes, *Nano Res.* **2009**, *2*, 599.
[140] H. Qiu, Y. Maeda, T. Akasaka, *J. Am. Chem. Soc.* **2009**, *131*, 16529.
[141] X. Tu, S. Manohar, A. Jagota, M. Zheng, *Nature* **2009**, *460*, 250.
[142] H. Zhang, Y. Liu, L. Cao, D. Wei, Y. Wang, H. Kajiura, Y. Li, K. Noda, G. Luo, L. Wang, J. Zhou, J. Lu, Z. Gao, *Adv. Mater.* **2009**, *21*, 813.
[143] A. L. Antaris, J.-W. T. Seo, A. A. Green, M. C. Hersam, *ACS Nano* **2010**, *4*, 4725.
[144] S. Ghosh, S. M. Bachilo, R. B. Weisman, *Nat. Nanotechnol.* **2010**, *5*, 443.
[145] E. H. Hároz, W. D. Rice, B. Y. Lu, S. Ghosh, R. H. Hauge, R. B. Weisman, S. K. Doorn, J. Kono, *ACS Nano* **2010**, *4*, 1955.
[146] D. Nishide, H. Liu, T. Tanaka, H. Kataura, *Phys. Status Solidi B* **2010**, *247*, 2746.
[147] T. Tanaka, Y. Urabe, D. Nishide, H. Liu, S. Asano, S. Nishiyama, H. Kataura, *Phys. Status Solidi B* **2010**, *247*, 2867.
[148] Y. Feng, Y. Miyata, K. Matsuishi, H. Kataura, *J. Phys. Chem. C* **2011**, *115*, 1752.
[149] T. Tanaka, Y. Urabe, D. Nishide, H. Kataura, *J. Am. Chem. Soc.* **2011**, *133*, 17610.
[150] N. P. Bhatt, P. Vichchulada, M. D. Lay, *J. Am. Chem. Soc.* **2012**, *134*, 9352.
[151] B. S. Flavel, M. M. Kappes, R. Krupke, F. Hennrich, *ACS Nano* **2013**, *7*, 3557.
[152] C. Y. Khripin, J. A. Fagan, M. Zheng, *J. Am. Chem. Soc.* **2013**, *135*, 6822.
[153] R. Krupke, F. Hennrich, H. v. Löhneysen, M. M. Kappes, *Science* **2003**, *301*, 344.
[154] M. Zheng, A. Jagota, E. D. Semke, B. A. Diner, R. S. McLean, S. R. Lustig, R. E. Richardson, N. G. Tassi, *Nat. Mater.* **2003**, *2*, 338.
[155] M. S. Arnold, A. A. Green, J. F. Hulvat, S. I. Stupp, M. C. Hersam, *Nat. Nanotechnol.* **2006**, *1*, 60.
[156] G. Hong, M. Zhou, R. Zhang, S. Hou, W. Choi, Y. S. Woo, J.-Y. Choi, Z. Liu, J. Zhang, *Angew. Chem. Int. Edit.* **2011**, *50*, 6819.
[157] P. G. Collins, M. S. Arnold, P. Avouris, *Science* **2001**, *292*, 706.
[158] S. H. Jin, S. N. Dunham, J. Song, X. Xie, J.-h. Kim, C. Lu, A. Islam, F. Du, J. Kim, J. Felts, Y. Li, F. Xiong, M. A. Wahab, M. Menon, E. Cho, K. L. Grosse, D. J. Lee, H. U. Chung, E. Pop, M. A. Alam, W. P. King, Y. Huang, J. A. Rogers, *Nat. Nanotechnol.* **2013**, *8*, 347.
[159] K. Seo, C. Kim, Y. S. Choi, K. A. Park, Y. H. Lee, B. Kim, *J. Am. Chem. Soc.* **2003**, *125*, 13946.
[160] G. Zhang, P. Qi, X. Wang, Y. Lu, X. Li, R. Tu, S. Bangsaruntip, D. Mann, L. Zhang, H. Dai, *Science* **2006**, *314*, 974.
[161] K. Maehashi, Y. Ohno, K. Inoue, K. Matsumoto, *Appl. Phys. Lett.* **2004**, *85*, 858.
[162] J. W. Song, H. W. Seo, J. K. Park, J. E. Kim, D. G. Choi, C. S. Han, *Curr. Appl. Phys.* **2008**, *8*, 725.
[163] Y. Hu, Y. Chen, P. Li, J. Zhang, *Small* **2013**, *9*, 1306.
[164] F. Ding, A. R. Harutyunyan, B. I. Yakobson, *Proc. Natl. Aacd. Sci. USA* **2009**, *106*, 2506.
[165] H. Dumlich, S. Reich, *Phys. Rev. B* **2010**, *82*, 085421.
[166] S. Bandow, S. Asaka, Y. Saito, A. M. Rao, L. Grigorian, E. Richter, P. C. Eklund, *Phys. Rev. Lett.* **1998**, *80*, 3779.
[167] R. Rao, D. Liptak, T. Cherukuri, B. I. Yakobson, B. Maruyama, *Nat. Mater.* **2012**, *11*, 213.
[168] S. M. Bachilo, L. Balzano, J. E. Herrera, F. Pompeo, D. E. Resasco, R. B. Weisman, *J. Am. Chem. Soc.* **2003**, *125*, 11186.
[169] W.-H. Chiang, R. Mohan Sankaran, *Nat. Mater.* **2009**, *8*, 882.
[170] M. He, H. Jiang, E. I. Kauppinen, J. Lehtonen, *Nanoscale* **2012**, *4*, 7394.
[171] B. Wang, C. H. P. Poa, L. Wei, L.-J. Li, Y. Yang, Y. Chen, *J. Am. Chem. Soc.* **2007**, *129*, 9014.
[172] X. Yu, J. Zhang, W. Choi, J.-Y. Choi, J. M. Kim, L. Gan, Z. Liu, *Nano Lett.* **2010**, *10*, 3343.
[173] R. E. Smalley, Y. Li, V. C. Moore, B. K. Price, R. Colorado, H. K. Schmidt, R. H. Hauge, A. R. Barron, J. M. Tour, *J. Am. Chem. Soc.* **2006**, *128*, 15824.
[174] Z. Ren, *Nat. Nanotechnol.* **2007**, *2*, 17.
[175] J. Liu, C. Wang, X. Tu, B. Liu, L. Chen, M. Zheng, C. Zhou, *Nat. Commun.* **2012**, *3*, 1199.
[176] K. H. Liu, X. P. Hong, Q. Zhou, C. H. Jin, J. H. Li, W. W. Zhou, J. Liu, E. G. Wang, A. Zettl, F. Wang, *Nat Nanotechnol* **2013**, *8*, 917.
[177] Y. B. Chen, Y. Hu, M. X. Liu, W. G. Xu, Y. F. Zhang, L. M. Xie, J. Zhang, *Nano Lett.* **2013**, *13*, 5667.
[178] N. Hamada, S. Sawada, A. Oshiyama, *Phys. Rev. Lett.* **1992**, *68*, 1579.
[179] M. S. Dresselhaus, G. Dresselhaus, R. Saito, *Carbon* **1995**, *33*, 883.
[180] H. Kataura, Y. Kumazawa, Y. Maniwa, I. Umezu, S. Suzuki, Y. Ohtsuka, Y. Achiba, *Synthetic Met.* **1999**, *103*, 2555.
[181] A. Jorio, R. Saito, J. H. Hafner, C. M. Lieber, M. Hunter, T. McClure, G. Dresselhaus, M. S. Dresselhaus, *Phys. Rev. Lett.* **2001**, *86*, 1118.
[182] S. M. Bachilo, M. S. Strano, C. Kittrell, R. H. Hauge, R. E. Smalley, R. B. Weisman, *Science* **2002**, *298*, 2361.
[183] M. Y. Sfeir, F. Wang, L. M. Huang, C. C. Chuang, J. Hone, S. P. O'Brien, T. F. Heinz, L. E. Brus, *Science* **2004**, *306*, 1540.
[184] C. S. Allen, C. Zhang, G. Burnell, A. P. Brown, J. Robertson, B. J. Hickey, *Carbon* **2011**, *49*, 4961.
[185] J. W. G. Wildoer, L. C. Venema, A. G. Rinzler, R. E. Smalley, C. Dekker, *Nature* **1998**, *391*, 59.
[186] M. S. Dresselhaus, G. Dresselhaus, R. Saito, A. Jorio, *Phys. Rep.* **2005**, *409*, 47.
[187] L. J. Ci, L. Song, D. Jariwala, A. L. Elias, W. Gao, M. Terrones, P. M. Ajayan, *Adv. Mater.* **2009**, *21*, 4487.